Award Number: W81XWH-10-2-0065

TITLE: Biomedical analyses, tolerance, and mitigation of acute and chronic trauma

PRINCIPAL INVESTIGATOR: Dr. Frank A. Pintar

CONTRACTING ORGANIZATION: The Medical College of Wisconsin, Milwaukee, WI 53225

REPORT DATE: July 2012

TYPE OF REPORT: Annual

PREPARED FOR: U.S. Army Medical Research and Materiel Command
Fort Detrick, Maryland 21702-5012

REPORT DOCUMENTATION PAGE

Form Approved
OMB No. 0704-0188

1. REPORT DATE *(DD-MM-YYYY)*	2. REPORT TYPE	3. DATES COVERED *(From - To)*
01-07-2012	Annual	1 JUL 2011 - 30 JUN 2012

4. TITLE AND SUBTITLE
Biomedical analyses, tolerance, and mitigation of acute and chronic trauma

5a. CONTRACT NUMBER

5b. GRANT NUMBER
W81XWH-10-2-0065

5c. PROGRAM ELEMENT NUMBER

6. AUTHOR(S)
Dr. Frank A. Pintar

E-Mail: fpintar@mcw.edu

5d. PROJECT NUMBER

5e. TASK NUMBER

5f. WORK UNIT NUMBER

7. PERFORMING ORGANIZATION NAME(S) AND ADDRESS(ES)
The Medical College of Wisconsin
Milwaukee, WI 53225

8. PERFORMING ORGANIZATION REPORT NUMBER

9. SPONSORING / MONITORING AGENCY NAME(S) AND ADDRESS(ES)
U.S. Army Medical Research and Materiel Command
Fort Detrick, Maryland 21702-5012

10. SPONSOR/MONITOR'S ACRONYM(S)

11. SPONSOR/MONITOR'S REPORT NUMBER(S)

12. DISTRIBUTION / AVAILABILITY STATEMENT
Approved for Public Release; Distribution Unlimited

13. SUPPLEMENTARY NOTES

14. ABSTRACT

The objective of this multidisciplinary effort is to comprehensively investigate and develop objective tools to evaluate and mitigate injuries to military personnel from different types of primary mechanical loading and secondary trauma due to the initial insult. Loading situations may include external force applications simulating blast, vehicle impact, and single- and multi-cycle longitudinal load applications to the human body. The research is in progress. Literature reviews have provided specific directions for future experimental design. Tests conducted on the Hybrid-III ATD with both curved and straightened lumbar spines demonstrated that forces further away from the source of impact were less sensitive to changes in impact pulse configuration. An in vivo animal study is under way to compare two different artificial disc surgical interventions against the current standard of care, bony fusion. PMHS studies were done to assess lumbar spine fracture under vertical seat-pan loading. Studies indicated that acceleration pulse is a critical determinant of what body region fractures. Softer seats that generate a sigmoid pulse to the pelvis may protect the pelvis but contribute to lumbar spine fracture risk. Seat pan force magnitude may not be a good indicator of pelvis fracture.

15. SUBJECT TERMS
Cervical Spine Degeneration, Cervical Artificial Disc, Lumbar Spine Injury

16. SECURITY CLASSIFICATION OF:			17. LIMITATION OF ABSTRACT	18. NUMBER OF PAGES	19a. NAME OF RESPONSIBLE PERSON
a. REPORT	b. ABSTRACT	c. THIS PAGE			USAMRMC
U	U	U	UU	43	19b. TELEPHONE NUMBER *(include area code)*

TABLE of CONTENTS

INTRODUCTION

The objective of this multidisciplinary effort is to comprehensively investigate and develop objective tools to evaluate and mitigate injuries to military personnel from different types of primary mechanical loading and secondary trauma due to the initial insult. Loading situations may include external force applications simulating blast, vehicle impact, and single- and multi-cycle longitudinal load applications to the human body. The approach consists of using tools such as clinical analyses to understand the epidemiology and injury-related outcomes, in vitro experiments using Post Mortem Human Subject (PMHS) materials and in vivo experimental animal models, physical models such as the federalized Hybrid III anthropomorphic test device (ATD) and advanced dummies such as the THOR dummy of various sizes, computational tools such as finite element models, and a careful syntheses of these data.

The scope of the current effort was directed toward assessing the most current treatments for cervical spine degenerative disorders including biomechanical assessment of artificial discs. The research efforts used a combination of literature searches, computational modeling, and an in vivo animal model. The research efforts were also directed toward understanding lumbar spine injury in the military environment by designing a test apparatus for use on an acceleration sled simulating vertical loading up the spinal column. The test setup was exercised to determine effect of loading rate on spinal load transmission for different types of ATD designs compared to PMHS.

Special Administration Note: The human cadaver studies proposed in this investigation were subject to approval by the Army's Office of Research Protections. We received what we thought was an approval letter dated 28 July 2011 and began testing. A few months later we were told by the same office that a new policy was being drafted and a new approval was required. The new policy required a complete change in the donor consent process that we now have complied with. We have submitted all new materials and await new approvals. Some of the research has been on hold because of these new Army policy decisions.

BODY of REPORT

Progress on Tasks:

TASK 1 LITERATURE REVIEWS

Literature reviews on cervical spine surgical interventions; cervical spine disease and degeneration, lumbar spine injury criteria, and cervical spine injury criteria have been completed and submitted to the USAARL. An excerpt from the review on cervical spine injury criteria is provided below.

Review of Cervical Spine Injury Criteria

Introduction

The cervical spinal column consists of several bones interconnected by soft tissues such as intervertebral discs, ligaments and muscles, and maintains the integrity of the neck in physiological and traumatic environments. Injuries resulting in instability to the cervical spine or loss of normal function from excessive deformations secondary to external dynamic forces such as those encountered in falls, motor vehicle crashes, sports-related events, and military environments can have significant consequences. Mechanically-induced traumas are transmitted to the cervical spine in different ways. For example, dynamic and unintentional head contact loading during occupant motions in military environments can result in excessive loads (forces and bending moments) to the neck structure. Axial or eccentric compressive forces transmitted to the cervical spine may result in fracture, lead to spinal instability, and impair solider function, in addition to long-term consequences such as enhanced degenerative disorders. This literature review examines current biomechanical fracture tolerance and injury criteria using post mortem human surrogate experiments. Due to an almost paucity of studies specific to military applications, tests and results from other areas such as motor vehicle environments are included in the review.

Previous injury biomechanics research

Loading issues: Conventional loading methods used in the study of human tolerance to cervical spine injuries include: drop tests, impacts with pendulum apparatus, and dynamic loads applied to intact PMHS using acceleration/deceleration or Hyge sled equipment, and electro-hydraulic testing devices.

Drop tests: Dynamic loading is applied by dropping chosen experimental models (osteo-ligamentous cervical spine-head preparations, isolated spine segments, or intact PMHS) onto different surfaces or targets with varying geometry and padding/stiffness (3-5). These tests induce dynamic compressive forces in addition to the off-axis and coupled forces and moments depending on specimen factors such as alignment, added torso mass, and restraint system simulation. These “free-fall” tests provide data such as force, deflection and, acceleration. Depending on the region of impact and the boundary condition, in an intact PMHS model, overall motions of the cervical spine can be recorded using retro-reflective markers inserted to the tips of spinous processes, as these are the prominent and protruding components of the human cervical spine. In the past, high-speed films have been analyzed to determine head-neck motions and influence of shoulder contact timing, neck loading and injury (3, 4). Isolated oseto-ligamentous column drops can be instrumented with deformation sensors such as a strain gages or accelerometers at specific vertebra to monitor local kinematics and use for defining injury risk curves. However, local buckling and or out-of-plane motions subsequent to initial injury may introduce spinal instability, add to severity of trauma, confound injury metrics, mechanisms, and risk curves. Despite this short coming, drop tests cans be used to derive biofidelity corridors for manikin evaluations.

Tests with pendulum apparatus: The pendulum device applies dynamic loads to experimental models (head-neck complexes or intact PMHS) using an impacting surface at its leading face (6-9). The impacting mass can be varied to modulate the applied acceleration-time pulse or velocity profile. Local dynamic contact with the impacting surface induces compressive forces in addition to the off-axis and coupled forces and moments depending on specimen factors such as alignment. These tests provide data such as applied force, deflection, and acceleration. In addition, similar to drop tests, specimens can be instrumented with retro-reflective markers to obtain kinematic information. High-speed films have been analyzed to determine head-neck motions and injury mechanisms. Depending on the experimental model, sensors such as a strain gages or accelerometers can be used to obtain vertebral kinematics for defining injury risk curves. Tolerance information of specific components is difficult to derive if intact cervical column-head preparations are used as the actual loading sustained by the component are not known. However, this method can be more effectively used to derive biofidelity corridors for manikin evaluations.

Tests with sled equipment: The sled loading device applies acceleration/deceleration loading using sled equipment to intact PMHS or in some cases, specially prepared head-neck complexes (10, 11). Modern sleds have the ability to modulate the applied acceleration-time pulse histories and velocity profiles, both in terms of magnitude and duration. Specimens can be instrumented, as above, with retro-reflective markers and accelerometers to obtain head-neck kinematic information. Inertial loading to the head-neck can be applied using this device. It is possible to derive upper and lower neck loads using head accelerations, kinematic of the head and thoracic spine and, physical properties of the head including mass, center of gravity and moments of inertia. These PMHS sled experiments and processed data can be used to conduct match-pair tests and use in biofidelity evaluations. Also, presence or absence of cervical spine injuries can be used along with neck loads (forces and moments) to derive risk curves. As the experimental model involves the entire and sled loading, the number of repeated tests is generally limited. In addition, it is difficult to extract spinal segment/level-specific forces and moments and extract risk curves from sled tests.

Tests with electro-hydraulic device: These devices apply the external dynamic loading using the piston of the electro-hydraulic testing device to different types of experimental models: from intact PMHS, specially prepared head-neck complexes, isolated functional units, and components such as vertebral bodies (12-20). Custom devices have the ability to apply axial tensile or compressive forces high rate of loading, up to 9 m/s, to the above models. Because the piston travel is uniaxial, in order to accomplish different loading modes, it is necessary to orient the specimen under test appropriately. For example, to apply compression-flexion loading to a straightened or pre-flexed head-neck complex, the piston should be aligned such that the occipital condyles are posterior to the piston axis/travel. Likewise, in order to apply compression-extension loading, the line of the loading axis should be posterior to the occipital condyles. Control of piston travel defines velocity, excursion defines specimen displacement, and time duration modulates pulses characteristics. Specimens can be instrumented, with retro-reflective markers and accelerometers to obtain head-neck kinematic information. As in the case of sled tests, It is possible to derive neck loads using head accelerations, kinematic of the head and thoracic spine and, physical properties of the head. Likewise, match-pair tests and biofidelity evaluations can be conducted. Injuries cane correlated with neck loads to derive risk curves. However, it is difficult to achieve a constant velocity as the piston has to initiate its travel from rest, and at the point/level of peak displacement, unloading has to initiate. Also, the inertial effects of the piston need compensation for force measurements.

Specimen details

Different types of experimental models exist to determine the biomechanical properties, replicate field injuries, derive injury mechanisms, and determine human tolerance in terms of variables such as forces and risk curves using the above described loading apparatuses. Models range from: isolated tissues such as vertebral bodies and ligaments, to functional units (single and multiple level), to ligamentous columns without head and with intact or artificial head, to intact PMHS.

Isolated components: These types of experimental models are used to delineate the material properties of the specific component (example, vertebral bodies) and understand tolerance characteristics. Vertebral body tests have been conducted using electro-hydraulic testing devices. Generally, the vertebral body under test is fixed at the superior and inferior ends in poly-methyl-methacrylate and the surfaces are maintained horizontal to apply uniform axial compressive loads from an electro-hydraulic testing device or Instron apparatus. Pretest geometrical measurements and anatomical images are obtained, specimen is loaded at a constant force or displacement rate to pre-defined strain level (often one-half), and unloaded. Relaxation properties can be obtained if the peak applied strain is low. Posttest anatomical images re obtained. In addition to the applied force and displacement records from the testing device, a six-axis load cell placed underneath the preparation will allow record of transmitted forces and moments. Optical techniques can be used to determine local strains. Engineering stress-strain can be derived from these data providing material properties and failure patterns from images. Similar methodology can be used for testing intervertebral discs, using one-level vertebra-disc-vertebra (functional unit) to vertebral body-disc-vertebral body (disc segment) models. By suitably orienting the disc model, shear, tensile, and compressive mechanical properties can be determined at dynamic rates and injury risk curves can be derived under different modes, at spinal levels and at different anatomical regions. In essence these tests provide gross biomechanical response curves. Isolated components tests have been conducted using soft tissues such as ligaments under tensile loading. In order to determine the gross mechanical properties of spinal ligaments, in situ procedures have been adopted. These involve isolating the ligament under test (example, anterior longitudinal ligament) while maintaining its bony attachments intact, i.e., bone-ligament-bone preparations. In situ tests have shown that the methodology produces clinical injuries such as tears of the mid-substance more often than avulsions under dynamic loading. Localized deformation (and strain) data can also be obtained using optical techniques. These tests can delineate the responses and failure risk curves as function of level and type of ligament. Intervertebral annulus can also be tested by using “coupons” to determine the regional and level-specific properties and risk curves.

Segmented columns: These types of experimental models are used to delineate the gross biomechanical responses of the spine at a more macro level, and determine tolerance characteristics. Because more than one functional unit is used, effects of spinal curvature and pre-alignment issues to control for posture are automatically incorporated into the experimental model. However, the degree of inclusion of these factors depends on the number of segments. Consequently, these models tend to be more realistic from injury reproduction perspectives although failure responses of individual components cannot be quantified because the load-path at a segmental level is unknown. Motions of the various intervertebral levels can be obtained optically at high rates of 1000 samples per second. Likewise, local accelerations and strains of individual vertebrae can obtained using accelerometers and strain gages to determine the time of fracture or spinal instability. Positioning the segmented column on an x-y cross table mounted to the platform of an electro-hydraulic testing device is needed to achieve the intended posture or pre-alignment. Pre-load simulating head and protective equipment mass (and other physical properties) can be applied to the superior end of the fixation, although it is difficult to

mimic the inertial properties of the head-helmet system with continued application of the dynamic load from the piston of the testing device. The transmitted forces and moments can be recorded at the inferior end using a six-axis load cell. Forces and moments at the segmental level of injury may be estimated although the local dynamics are not known. High-speed video images can be taken to document macroscopic failures, high-speed x-rays can be obtained for bony fractures, and localized segmental motions analyses can be performed using this model. Furthermore, biofidelity tests can be conducted using match-pair approach.
Another methodology to apply dynamic loads to the segmented column is using free-fall or drop techniques. This involves fixing the ends of the column, applying preloads (if any), controlling alignment by techniques such as pre-flexing using cables, and dropping on to targets with known stiffness to modulate the pulse. As indicated earlier, ensuing motions of the column following initial contact with the target may induce parasitic loads and contribute to additional injuries. However, these tests can also be used to conduct match-pair tests and evaluate manikin biofidleity.

Intact head-neck complexes: This is a special case of segmented columns, wherein instead of simulating the head and the protective equipment with its at-rest (static) physical properties, intact head is used. The advantage is that it will not compromise the integrity of the base of the skull to upper neck junction and maintains the center of gravity and inertial properties throughout the loading process. This model has the ability to also automatically accommodate the passive musculature of the neck including the sub-occipital complex and the portions of the trapezius, structures difficult to include in segmented column preparations. However, additional procedures are necessary to maintain the initial stability to the head-neck complex as the head mass is considerably greater than the neck. While superior to inferior loading (from head to neck) can be easily applied using the electro-hydraulic or Instron devices at dynamic rates, the head-neck preparation needs to be inverted if drop tests are the loading method of choice. Under this choice, the internal static loading of the intervertebral joints do not mimic the in vivo human because of the inverted nature, this likely confounding the biomechanical outcomes. Other factors such as alignment, instrumentation, data and injury analyses follow the same procedures, described above for segmented columns.

Intact PMHS: This is the closet experimental model to test the head-neck system as the rigidity assumption used in the segmented and intact head-neck models is relaxed and full integrity is maintained of the cervico-thoracic spine junction and associated musculature. However, positioning and loading of the intact PMHS is difficult. Drop tests often have little control due to continuing motions of the large torso and inferior body mass acting as soon as the inverted PMHS head contacts the target. Electro-hydraulic devices are not always amenable to accommodate the entire PMHS as special seating and restraining procedures are needed, in addition to stabilizing the head mass with an intact preparation. Optical monitoring of segmental motions is also difficult as placement of targets on to bony surfaces in the cervical spinal column surrounded by musculature and other soft tissues are challenging. The maintenance of preposition/posture is also difficult with this model. However, pendulum impact tests can be conducted with more ease. The intact PMHS can be placed supine on a table to allow impacts to selected regions of the head, the impacting surface can be prepared with different targets to induce specific pulses, and it is possible to monitor the overall motions of the head with respect to the T1 junction as the specimen is supine. However, the preparation is devoid of the natural axial superior to inferior loading of the intervertebral joints. In addition, intervertebral joints, vertebrae and discs are under the antero-posterior directed self-weight, another non-physiological condition in pendulum tests. Seated PMHS subjected to pendulum impacts share similar pros and cons to tests with the electro-hydraulic testing device. Many of these difficulties are obviated by resorting to sled tests wherein the PMHS is seated with

restraints, oriented in the Frankfurt plane, and the acceleration pulse is applied instead of a direct loading through the piston or pendulum. Hence, intact PMHS are more amenable to sled testing methods. Furthermore, match-pair tests can be conducted with the whole manikin for biofidelity evaluations.

Human data: peak metrics, response corridors, and injury risk curves

Laboratory tests aimed to determine the injury biomechanics have used conventional radiography, CT scanning, detailed autopsy and cryomicrotomy techniques to identify and document trauma to bones, ligaments and intervertebral joints. PMHS models are not suitable for magnetic resonance imaging and furthermore, CT is a better imaging tool for assessing bony abnormalities. Repeated testing protocols need clinical evaluations in addition to intermediate x-rays to ensure both bony and soft tissue/joint integrity evaluations. From quantified data perspectives, as indicated in earlier sections, different devices have different capabilities to record biomechanical outcome measures. Commonly, drop tests include input height quantifying the impact velocity, six-axis loads sustained by the specimen with a stationary load cell placed on the platform of the drop tower device, local accelerations of vertebrae and two-dimensional kinematics of the joints and bones, often in the mid-sagittal plane. In contrast, pendulum tests often record the impact force from a load call and accelerations from an accelerometer to account for inertia effects, as input metrics. Specimen-specific biomechanical metrics may include kinematics and injury assessments. Tests using the electro-hydraulic device record the piston force, acceleration, and displacement using a force gage, uniaxial accelerometer, and linear variable differential transducer as input variables. Sled tests measure the applied acceleration pulses using an accelerometer located on its platform as the input. Specimen-specific instrumentations depend on the type of models used in these devices.

In general, for determining human tolerance and injury risk curves specimen factors such as age and gender are considered along with peak force, acceleration, displacement, and derived variables such as energy and stiffness. Commonly accepted methods use logistic regression, Weibull distribution, and survival analyses. Because of limitations in sample size, a considerable majority of studies have only provided specimen-specific or mean and standard deviation data in published literature. As can be appreciated in the following, injury risk curves for different types of cervical spine traumas are not differentiated based on rate. Furthermore, reproduction of traumas at high rates encountered in military environments and specific to the UBB application have been extremely limited. A chronological review of some papers focusing on impact loading test are presented. Attention is focused on injuries and tolerance metrics. Tests were conducted using intact PMHS and component models to identify and document injuries, derive injury mechanisms, and suggest tolerance metrics.

Intact PMHS tests: Pendulum impact tests: In an earlier study, 11 tests were conducted with a pendulum at velocities ranging from 6.8 to 10.2 m/s (6). Supine positioned specimens were subjected to vertex loading using a 9.9 kg padded impacting surface. Three specimens sustained no injuries while fractures of various components of all sub-axial cervical vertebrae (C2 to C7) were reported. Fracture thresholds were reported to be associated with peak force, velocity, and energy of 5.7 kN, 7.5 m/s, and 380 Nm. Spine posture or alignment was attributed to be a factor in injuries, injury mechanisms, and tolerance. Nineteen intact PMHS were subjected in a later study to axial impacts using the same horizontal impacting device (7, 8). Five specimens were tested at a sub-failure loading corresponding to 8 m/s with forces ranging from 3.93 to 4.8 kN and pulse widths ranged from 12 to 17 m/s. The remaining 14 specimens were tested at velocities ranging from 6.9 to 10.9 m/s. The 10 kg pendulum impacting surface was padded. Unlike the previous study, based on some approximation regarding physical properties of the head, neck loads were derived at the head-neck junction for sub-failure

experiments. In the failure dataset, at autopsy, four specimens sustained no injuries, two sustained skull fractures only, and the remaining eight demonstrated cervical vertebra fractures and soft tissue injuries at all sub-axial levels. The study found that peak forces as low as 3 kN results in cervical spine fracture while forces up to 16 kN did not result in fracture. It was concluded that peak impact force and head injury criterion (HIC) were not reliable predictors of cervical spine injury while maximum head velocity and time integral of applied impact force correlated with spine injury (not statistical). In another study, a pendulum mass of 56 kg was used to deliver impacts to the vertex of 12 intact PMHS (9). As in the previous studies, injuries were identified at subaxial segments in the form of fractures, dislocations and disc ruptures. At velocities ranging from 4.6 to 5.6 m/s, peak forces ranged from 1.8 to 10.3 kN. The study concluded that posture or initial orientation is an important factor for injuries and injury mechanisms, head kinematics is not adequate to describe neck traumas, and the complex nature of spinal responses precludes the use of one criterion such as peak force to describe tolerance.

Drop tests: Eight intact PMHS were dropped from 0.1 to 1.8 m such that the vertex of the head contacted a force plate positioned to measure axial and shear forces (5). The force plate was covered with padding and multiple impacts were conducted. The specimens were aligned such that in one group the heads were constrained to rotate in the mid-sagittal line and in the other group head was angulated about all three the anatomical axes to investigate the postural effects. Injuries at all cervical levels (C1 to C7) were identified at autopsy. The study concluded that flexion-type damage is unlikely if the head is constrained about mid-sagittal plane while preposition is needed to incur this type of injury. These experiments produced fractures similar to those from pendulum tests, i.e., flexion-compression in lower and extension-compression in upper cervical segments. In another series of drop tests, 15 intact PMHS were subjected to vertex impact with head unrestrained and restrained boundary conditions (4). The initial pre-flexion of the head was achieved by a tether to achieve the constrained effects on head-neck loading. Restrained and unrestrained tests resulted in peak head forces ranging from 9.8 to 14.7 kN and 3.0 to7.12 kN, respectively. Neck injuries (C1-C7) were more common in the restrained than in the unrestrained groups indicating the role of posture on trauma. Uniaxial force gages introduced into the C5-C6 intervertebral disc space registered peak loads ranging from 1.1 to2.6 and 1.1 to1.8 kN in the unrestrained and restrained groups.

Electro-hydraulic piston tests: Three intact human PMHS were subjected to dynamic loading ranging from 1.12 to 1.42 m/s with the specimen positioned on the platform of the testing device (12). At piston displacements ranging from 3.6 to 9.2 cm, injuries were identified to C1 and C2 segments when the specimen was axially loaded (sample size two), while injuries to the C4-C6 segments were identified with the one specimen which was pre-extended before applying the compressive force.

An examination of results from the above discussed drop-, pendulum-, and electro-hydraulic piston-based data from intact PMHS tests indicate that whole-body exposures to vertex impact results in cervical spine fractures at all levels including dislocations, disc, ligament and joint injuries at all segments, and from this perspective, load transmission from the vertex is an important path for neck injury. The association of head injuries seen in WIA and KIA groups may be simulated using this approach of applying contact loads to experimental models, intact PMHS or otherwise, to be discussed later. However, acknowledging that these studies had small sample sizes for the wide variations encountered during the experimental setup, intentional or otherwise, a consensus could not be reached in terms of the factor(s) defining human tolerance. Because of these limitations, injury risk curves cannot be derived from this literature. Consequently, these intact PMHS studies should be considered as a first step in the reproduction and quantification of cervical traumas. As can also be appreciated from these

studies, impact velocities ranged from 1.4 to 10.9 m/s, with a majority of tests conducted below 6 m/s.

Osteo-ligamentous column and head-neck complex tests: Electro-hydraulic piston tests: In a series of tests, ten head to cervical spinal columns were tested using an electro-hydraulic device with pre-alignment conditions ranging from pre-flexion to axial to pre-extension at quasi-static to 1.52 m/s (12). Injuries were identified from the atlas to C7 levels. Under vertex impacts, injuries included burst fracture of C5, compression fractures of C2, C3, and facet fractures and ligament disruptions of the lower cervical spine. Specimens pre-aligned anteriorly with respect to the direction of the piston sustained C1-C2 dislocations, C4-5 compression fractures associated with posterior column disruptions. In contrast, specimen aligned under pre-extension sustained avulsion fracture of C4 and disruption of anterior longitudinal ligament at the lower cervical spine, C5-6. In another series of experiments isolated oseto-ligamentous cervical columns from base of skull to the cervico-thoracic levels were subjected to compressive forces piston velocities ranging from 0.45 to 0.92 m/s (13). Injuries were produced to all segments and these authors provided peak force, piston displacement, stiffness and energy data. Injuries included upper cervical trauma in the form of C1 (Jefferson) and C2 fractures, and lower cervical trauma in the form of wedge fractures of C4-C6, compression fractures of C4-C5, and burst fractures of C3-C6 vertebrae. Like the previous study, this investigation also underscored the issue of alignment condition on trauma production (12). These authors continued to conduct tests with osteo-ligamentous columns to determine the effects of end conditions on injuries, injury mechanisms, and tolerance (14). Six preparations (four C1-T1 under pinned-pinned and two base of skull-T1 columns under fixed-pinned condition) were subjected to compressive forces from an electro-hydraulic piston under quasi-static loading rates. All failure tests were conducted in “compression-flexion.” Shear forces were low in both end conditions, and failures were due to the combined axial force and sagittal bending moment. Pinned-pinned end conditions produced posterior ligament disruptions with minor wedging of bodies, while fixed-pinned conditions resulted in anterior and posterior column injuries. As expected, axial forces were lower in the pinned end condition tests. Differences in the moment-rotations responses were noted from 0.1 to 10 Hz between the PMHS and Hybrid III manikin, and the manikin response was stiffer than the PMHS at all rates.

Another series of tests were conducted using compressive loads at quasi-static and higher rates to osteo-ligamentous columns with the electro-hydraulic testing device. Tests at 2.5 mm/s loading rate from eight head-cervical columns aligned along the stiffest axis, as defined by pre-flexed posture (21), resulted in clinically seen injuries at all levels of the cervical spine (16, 18). Injury mechanisms were attributed to compression, compression-extension, and compression-flexion depending on the location, segment, and type of fracture, ligament and joint disruption. The authors also provided methods to analyze the local kinematic of vertebral segments using two-dimensional motion analyses using retro-reflective targets, which has become a norm in current biomechanical studies. The transient peaks and dips in the overall force-deflection and local kinematic biomechanical responses were used to describe segmental behaviors and explain local and mechanisms of injuries. Initiation of injuries as defined by local discontinuities in the responses manifesting as local yielding or micro-fracture/disruption of the integrity of the joint complex contributed to an improved understanding of the cervical spine response in compressive loading.

This methodology was extended to the dynamic domain in a subsequent study using the same pre-alignment condition along the stiffest axis and electro-hydraulic testing device (15, 22). In these investigations, experiments were conducted using nine specimens at higher rates, from 2.9 to 8.5 m/s. To achieve stability of the ligamentous head-neck complex devoid of neck musculature, the specimen was positioned using pulleys and deadweights in the anterior and

spring tension in the posterior regions of the preparation. The head was mounted in a neurosurgical stainless steel halo ring with fixation into the skull. The halo ring was fixed in the region of the occipital protuberance above the Frankfort plane. In the anterior region, two cables were passed through eye bolts bilaterally; the eye bolts were connected to the halo ring. Deadweights of 40 to 80 N were hung from these cables. In the posterior aspect of the preparation, a preloaded spring with a tension of 30 to 60 N was attached to the halo ring to simulate the posterior musculature. The head-neck complex was aligned so that the cervical spine assumed a normal flexed position by adjusting the spring tension and the anterior dead weight. Injuries sustained included vertebral body fractures of the mid-lower cervical spine (vertical, wedge, burst, and compression) associated with posterior element disruptions, and in addition, fractures of the spinous process were reported.

A more recent study combined data from earlier electro-hydraulic piston tests with pre-flexed head-neck complexes (age, 38-95 years; 10 females and 10 males) subjected to loading at rates up to 8 m/s (15-17, 23). Two statistical models were used to quantify the effects of loading rate, age and gender on maximum compressive force. The multiple linear regression model quantified the effects of the selected variables, while the survival-based proportional hazards quantified cervical spine injury risks. The authors preliminarily reported that increasing age reduces rate effects, especially at older age groups. At 4.5 m/s, the 50% probability of failure for the 50-year-old male spine was approximately 3.9 kN, emphasizing the likely need to scale based on age, especially for the military population. Although not illustrated in this review, the load carrying capacities of male spines were 600 N greater than those of female spines. This indicates the need for caution when combining data from males and females. The risk curve indicates that increasing rate increases the threshold and lower rate thresholds may be too conservative for situations such as those encountered in military vehicle operations. The authors concluded that the assessment of injury mechanisms, tolerance, and risk curves should be based on age, gender, and loading rates. In addition, these studies also provided data on human response corridors regardless of other variables such as age.

Drop tests: In a series of inverted drop tests, 22 specimens were prepared by attaching a 16 kg mass to the inferior end of the head-C7 column to simulate the torso mass, and fixing the T1 and T2 vertebrae in in a cup with polyester resin and C7-T1 disc was free (3, 24, 25). The specimens were dropped from a height of 0.4 to 0.61 m onto padded or rigid surfaces. The preparation was such that the specimens did not permit pre-flexion of the head-neck complex. Load cells at the distal inverted end of the preparation and at the base of the drop platform recorded the transmitted and applied forces at the head, respectively. A temporary decrease in the axial force recorded at the distal end with continued downward translation of the torso mass was used to define the onset of injury. Of the 22 impacts, 12 were padded and 10 were rigid surfaces, inclined at increments of 15 degrees from +30 (anterior impact) to -15 (posterior impact) degrees. Five of the 10 rigid impacts and one of the 12 padded impacts did not result in cervical spine injury. Injury mechanisms were attributed to belong to vertical compression, compression-extension, and distractive flexion/extension injuries were in the rigid group, and in addition to these, compression flexion injuries were added to the padded group. Head motion did not correspond to spine injuries in both groups of end conditions. Head rebound accounted for increased cervical spine loading, more in padded than rigid impacts. These results indicate that cervical spine mechanisms of injury are complex, non-straightened inverted cervical spines dropped at very similar heights with different end conditions produce multiple level, contiguous spinal injuries, demographic factors play a role in tolerance, and because of many variables additional studies are needed to clearly delineate human thresholds.

Table: Summary of data from inverted head-T1 column drop tests (*3, 24, 25*)

Condition	Unit	Impact type	
		Rigid	**Padded**
Velocity	m/s	2.43 to 3.12	3.03 to 3.51
Head force	N	5093 to 11621	1760 to 5963
Neck force	N	1971 to 4189	1289 to 4309
Neck force-axial	N	1552 to 2416	715 to 3172
Neck force-resultant	N	1593 to 2612	793 to 3509
Time between impact and injury	ms	2.2 to 8.3	14.0 to 30.5
Impulse	Ns	20.6 to 62.6	22.6 to 81.1
Sample size		10	12
Number of uninjured specimens		5	1

In another study, the sagittal bending moment parameter was included in addition to the vertical compressive force. Tests were done using 13 PMHS head neck complexes (27). The eccentricity of the applied vertical load from the piston, head impact force, neck force, sagittal bending moment at the injury level were used in data analyses. The eccentricity was defined as the horizontal distance between the center of the occipital condyles and the center of the T1 vertebral body, measured from the pre-test lateral radiograph. The peak vertical force from the distal six-axis load cell data defined the neck force. The sagittal bending moment at the injury site was determined using the load cell forces and moments and geometric relationships between the sensor and specimen, measured from pre-test radiographs and high-speed video images. The hyper-flexion injuries were classified as either minor (disruption of the lower cervical spine posterior ligament complex at one level) or major (extensive ligamentous injury usually with vertebral fractures and/or complete dislocations) injury groups. The two groups exhibited different cervical column kinematics in the sagittal plane. The minor injury group demonstrated a continuously forward rotational deformation of the cervical vertebrae with respect to T1 resulting in extreme hyper-flexion of one of the lower joints. Specimens with major injuries responded with column compression followed by local hyper-flexion at the injured level. Injuries depended on the posture/pre-alignment, quantified in terms of eccentricity. The eccentricities of all the tests ranged from 2.0 to 10.2 cm. The mean eccentricities of minor and major groups were 7.6 and 3.1 cm. Pre-alignment significantly influenced the mechanism of injury ($p<0.0001$), trauma rating ($p<0.005$), and fracture ($p<0.0001$) classification (28). Figure 19 shows the logistic distribution of hyper-flexion injury risk curves based on force and moment at the level of injury. These studies clearly indicate that posture affects biomechanical responses including spinal stability, injury mechanisms, scoring, peak metrics, response corridors and injury risk curves.

REFERENCES (used in above summary)

1. N. Yoganandan, F. A. Pintar, S. Larson, A. Sances, Eds., Frontiers in Head and Neck Trauma: Clinical and Biomechanical, (IOS Press, The Netherlands, 1998), pp. 743.
2. K. Vasquez, K. Logsdon, F. Brozoski, C. Chancey, “Warrior Injury Assessment Manikin (WIAMan) medical injury analysis” (U.S. Army Aeromedical Research Laboratory, Fort Rucker, AL, 2011).
3. R. Nightingale et al., in 41st Stapp Car Crash Conf. (Lake Buena Vista, FL, 1997), pp. 451-471.
4. N. Yoganandan et al., Experimental spinal injuries with vertical impact. Spine (Phila Pa 1976) 11, 855 (Nov, 1986).
5. G. Nusholtz, D. Huelke, P. Lux, N. Alem, F. Montalvo, in Biomechanics of Impact Injury and Injury Tolerances of Head-Neck Complex, S. Backaitis, Ed. (SAE, Warrendale, PA, 1983), vol. Publication #PT-43.

6. R. Culver, M. Bender, J. Melvin, “Mechanisms, tolerances, and responses obtained under dynamic superior-inferior head impact” (UM-HSRI-78-21, Michigan, 1978).
7. N. M. Alem, G. S. Nusholtz, J. W. Melvin, “Superior-inferior head impact tolerance levels” (UM-HSRI-82-21, Michigan, 1982).
8. N. M. Alem, G. S. Nusholtz, J. W. Melvin, in 28th Stapp Car Crash Conf. (1984), pp. 275-287.
9. G. S. Nusholtz, J. W. Melvin, D. F. Huelke, N. M. Alem, J. G. Blank, Response of cervical spine to superior-inferior head impact. 25th Stapp Car Crash Conf SAE paper #811005, 197 (1981).
10. F. A. Pintar, N. Yoganandan, D. J. Maiman, Lower cervical spine loading in frontal sled tests using inverse dynamics: potential applications for lower neck injury criteria. Stapp car crash journal 54, 133 (Nov, 2010).
11. N. Yoganandan, F. A. Pintar, J. Moore, D. J. Maiman, Sensitivity of THOR and Hybrid III dummy lower neck loads to belt systems in frontal impact. Traffic injury prevention 12, 88 (Feb, 2011).
12. D. J. Maiman et al., Compression injuries of the cervical spine: a biomechanical analysis. Neurosurgery 13, 254 (Sep, 1983).
13. J. H. McElhaney, B. J. Doherty, J. G. Paver, B. S. Myers, in Proc 27th Stapp Car Crash Conf. (Warrendale, PA, 1983), pp. 163-177.
14. J. H. McElhaney, B. J. Doherty, J. G. Paver, B. S. Myers, L. Gray, in Proc 32nd Stapp Car Crash Conf. (Warrendale, PA, 1988), pp. 21-28.
15. F. Pintar et al., in Stapp Car Crash Conf. (Orlando, FL, 1990).
16. F. Pintar et al., in 33rd Stapp Car Crash Conf. (Washington, DC, 1989), pp. 191-214.
17. F. Pintar et al., Dynamic characteristics of human cervical spine. SAE Transactions 104, 3087 (1995).
18. N. Yoganandan, F. A. Pintar, A. Sances, Jr., J. Reinartz, S. J. Larson, Strength and kinematic response of dynamic cervical spine injuries. Spine (Phila Pa 1976) 16, S511 (Oct, 1991).
19. N. Yoganandan, A. Sances, Jr., F. Pintar, Biomechanical evaluation of the axial compressive responses of the human cadaveric and manikin necks. Journal of biomechanical engineering 111, 250 (Aug, 1989).
20. N. Yoganandan et al., Injury biomechanics of the human cervical column. Spine (Phila Pa 1976) 15, 1031 (Oct, 1990).
21. Y. K. Liu, Q. G. Dai, The second stiffest axis of a beam-column: implications for cervical spine trauma. Journal of biomechanical engineering 111, 122 (May, 1989).
22. N. Yoganandan et al., Continuous motion analysis of the head-neck complex under impact. J Spinal Disord 7, 420 (Oct, 1994).
23. F. A. Pintar, N. Yoganandan, L. Voo, Effect of age and loading rate on human cervical spine injury threshold. Spine (Phila Pa 1976) 23, 1957 (Sep 15, 1998).
24. R. W. Nightingale, J. H. McElhaney, W. J. Richardson, T. M. Best, B. S. Myers, Experimental impact injury to the cervical spine: relating motion of the head and the mechanism of injury. J Bone Joint Surg Am 78, 412 (Mar, 1996).
25. R. W. Nightingale, J. H. McElhaney, W. J. Richardson, B. S. Myers, Dynamic responses of the head and cervical spine to axial impact loading. J Biomech 29, 307 (Mar, 1996).
26. B. L. Allen, Jr., R. L. Ferguson, T. R. Lehmann, R. P. O'Brien, A mechanistic classification of closed, indirect fractures and dislocations of the lower cervical spine. Spine (Phila Pa 1976) 7, 1 (Jan-Feb, 1982).
27. F. Pintar, L. Voo, N. Yoganandan, T. Cho, D. Maiman, in IRCOBI. (Boteborg, Sweden, 1998).
28. D. J. Maiman, N. Yoganandan, F. A. Pintar, Preinjury cervical alignment affecting spinal trauma. Journal of neurosurgery 97, 57 (Jul, 2002).
29. N. Yoganandan et al., Human head-neck biomechanics under axial tension. Medical engineering & physics 18, 289 (Jun, 1996).
30. C. A. Van Ee et al., Tensile properties of the human muscular and ligamentous cervical spine. Stapp car crash journal 44, 85 (Nov, 2000).
31. E. M. Yliniemi et al., Dynamic tensile failure mechanics of the musculoskeletal neck using a cadaver model. Journal of biomechanical engineering 131, 051001 (May, 2009).
32. S. H. Backaitis, H. J. Mertz, Eds., Hybrid III: The First Human-Like Crash Test Dummy, (Society of Automotive Engineers, Warrendale, PA, 1994), pp. 830.

33. H. J. Mertz, A. L. Irwin, P. Prasad, Biomechanical and scaling bases for frontal and side impact injury assessment reference values. Stapp car crash journal 47, 155 (Oct, 2003).
34. H. J. Mertz, P. Prasad, A. L. Irwin, in 41st Stapp Car Crash Conference. (1997).
35. M. Kleinberger, E. Sun, R. Eppinger, S. Kuppa, R. Saul, "Development of improved injury criteria for the assessment of advanced automotive restraint systems" (NHTSA, Washington, DC, 1998).
36. N. Rangarajan et al., in 16th International Conference on Enhanced Safety of Vehicles. (Windsor, Canada, 1998), pp. 1999-2010.
37. N. Yoganandan, F. A. Pintar, M. Schlick, J. Moore, D. J. Maiman, Comparison of head-neck responses in frontal impacts using restrained human surrogates. Annals of advances in automotive medicine / Annual Scientific Conference ... Association for the Advancement of Automotive Medicine. Association for the Advancement of Automotive Medicine. Scientific Conference 55, 181 (2011).
38. H. J. Mertz, in Accidental Injury: Biomechanics and prevention, A. M. Nahum, J. W. Melvin, Eds. (Springer, New York, 2002), pp. 72-88.

TASK 2: LUMBAR SPINE INJURY ASSESSMENT

A sled buck design has been finalized and tested under near-full constraints of the sled system. The design incorporates an adjustable seat back to allow for 25° flexion or extension of the torso, and also adjustment of the knee angle. The seat back is also adjustable vertically and is slotted to allow for high-speed camera viewing and quantitative motion capture of the lower spine region. The restraints are at the lap and lower leg and set to minimal tension to prevent flailing of the segments.

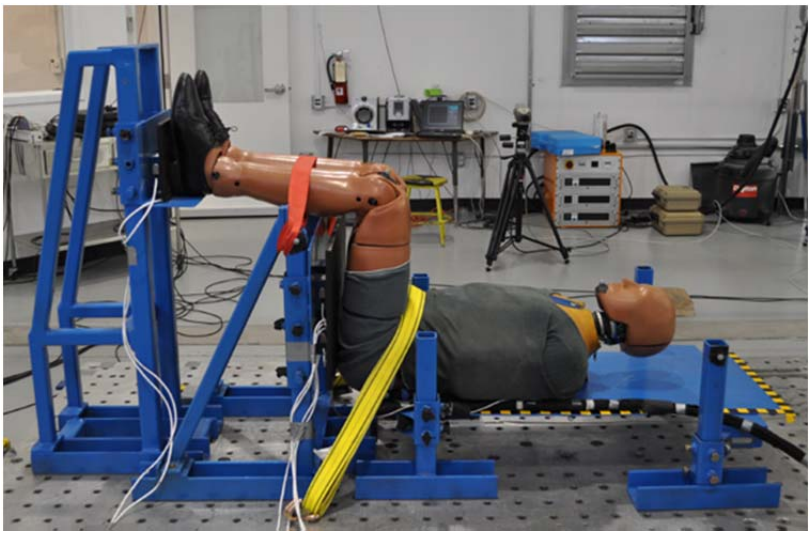

Almost 300 sled tests were conducted with dummies and PMHS that included a straight-spine DoTSID and 50th percentile male Hybrid III dummy. DoT SID has a straight and H3 has a kyphotic lumbar spine. More recently, the Army has provided a modified THOR test dummy for additional comparisons. Peak accelerations ranged from 6-56 G's and peak ΔV between 5 and 31 km/h. Onset rates ranged from 0.1 to 10 g/ms in a triangular input pulse. Axial forces from the foot pan, seat pan and upper neck were collected, along with spine accelerations at T1 and pelvis. Axial displacements of the visco-elastic lumbar components were also measured with retro-reflective markers placed along the spine at the lower thoracic and sacral regions. Preliminary analysis indicates a progressive time lag trend in biomechanical outputs from the

seat pan to pelvis to dorsal spine to neck and head. Point cloud plots, i.e., peak metric (example, seat pan acceleration as the ordinate) associated with its times of attainment were obtained for tests with sled acceleration peaks between 5 and 6 ms. As the lumbar spine of these dummies is considered to be stiffer than the human, the present results suggest that the time lag may be greater in the human than the dummy. This would imply a more gradual transfer of the external load to the rostral regions of the lumbar spine in the human. This issue along with continued data analyses will be explored using PMHS studies.

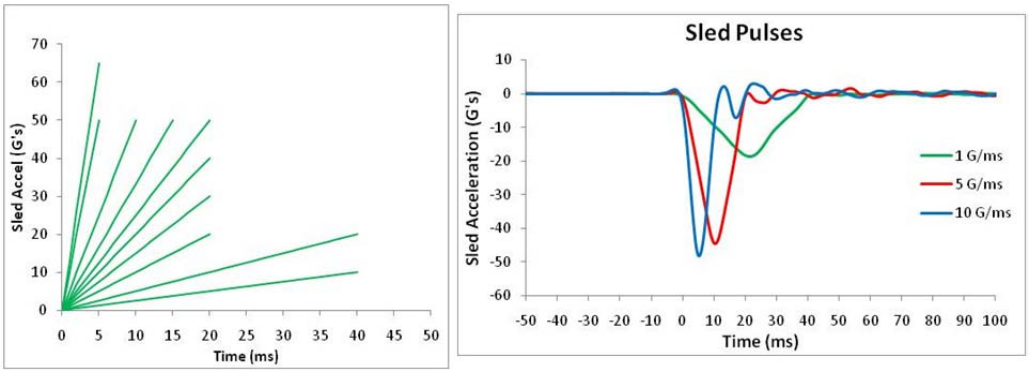

Left: sled acceleration versus time plots of the equipment used in the study. Right: specific time histories for three rates of onset.

Preliminary motion analysis of the axial movements in the lumbar region of the three surrogates is underway. 20 Vicon cameras were positioned laterally and above the sled to capture motions at 1000Hz. Retroreflective marker plates were affixed above and below the rubberized lumbar column in the Hybrid-3 and SID, and at the T-12 and sacrum in the PMHS via bone screws. Deflections are expressed as the superior segment relative to the inferior. The axial coordinate system is defined along the length of the seatback, with compression negative in polarity. Motion data for a matched-pair series of tests under a triangular pulse load of 30G peaking at 20ms is shown below. Lumbar axial displacement under this load is shown for a PMHS in a "neutral" supine position, the same PMHS in flexion, the Hybrid-3 dummy, and the straight spine SID. The figure below shows the load cell and motion analysis marker locations for the Hybrid-3 dummy.

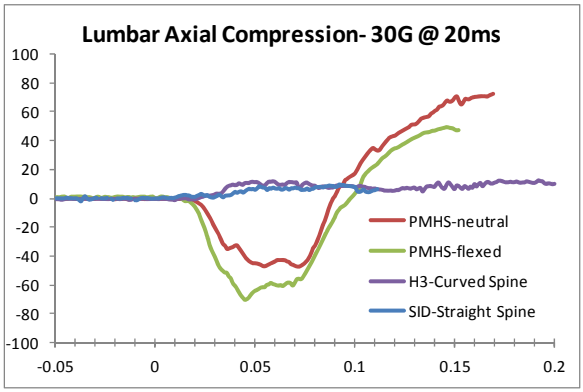

Lumbar axial compressions for H-3 curved spine SID straight spine, PMHS in neutral position, and PMHS in a flexed torso position. All were exposed to a 30G @ 20ms triangular pulse.

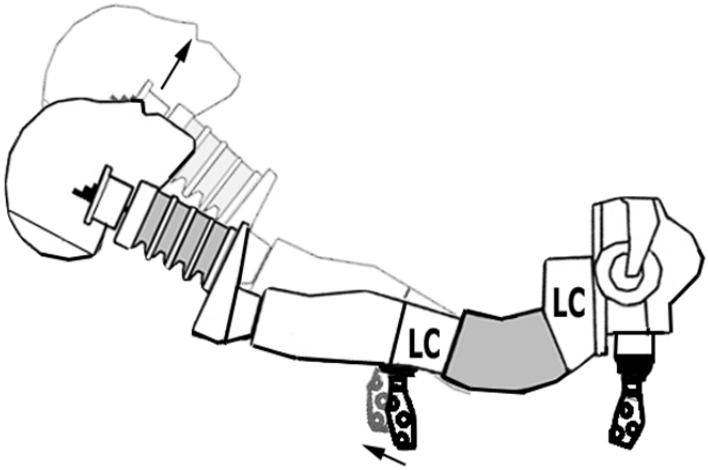

Lumbar load cell and motion analysis marker locations in the Hybrid-3 dummy.

The PMHS tests undergo a higher axial deflection compared to the much stiffer ATD lumbar column. Neither ATD experiences any compression, but they exhibit some distension due to the spreading of the markers while the torso undergoes flexion. The kyphotic curvature of the Hybrid-3 spine accentuates the effect as it flexes, compared to the straight spine in the SID dummy. The curvature of the spine also affects the response in the PMHS. A flexed positioning of the PMHS torso pre-test reduces the lordotic curvature in the lumbar region, and a greater compression results from axial alignment of the vertebrae with the direction of the applied pulse. The loads above and below the ATD lumbar column are also being addressed via newly acquired five and six axis load cells, respectively. A cephalic reduction in load of 7-10% is typical for the pulse shown and similar ones, however it is thought that wider pulses and/or lower rise times may result in transmission of the load more superiorly. The effect of pulse width on lumbar compression is shown in the below figure. For the same PMHS, a higher magnitude and shorter pulse results in less axial compression than for the 30G @ 20ms pulse in the flexed condition.

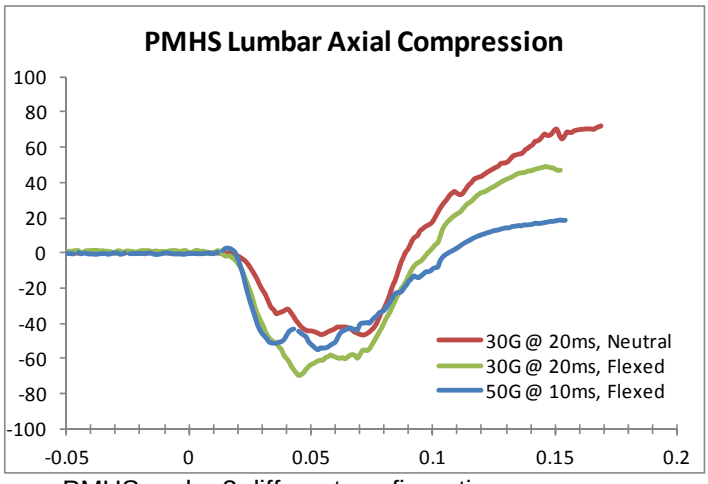

Lumbar deflections of the same PMHS under 3 different configurations.

Preliminary analysis of accelerations from the seat up to the head of the surrogate indicates a progressive time lag trend in biomechanical outputs from the seat pan to pelvis to dorsal spine to neck and head. As the lumbar spine of these dummies is considered to be stiffer than the human, the present results suggest that the time lag may be greater in the human than the dummy. This would imply a gradual transfer of the external load to the rostral regions of the lumbar spine in the human.

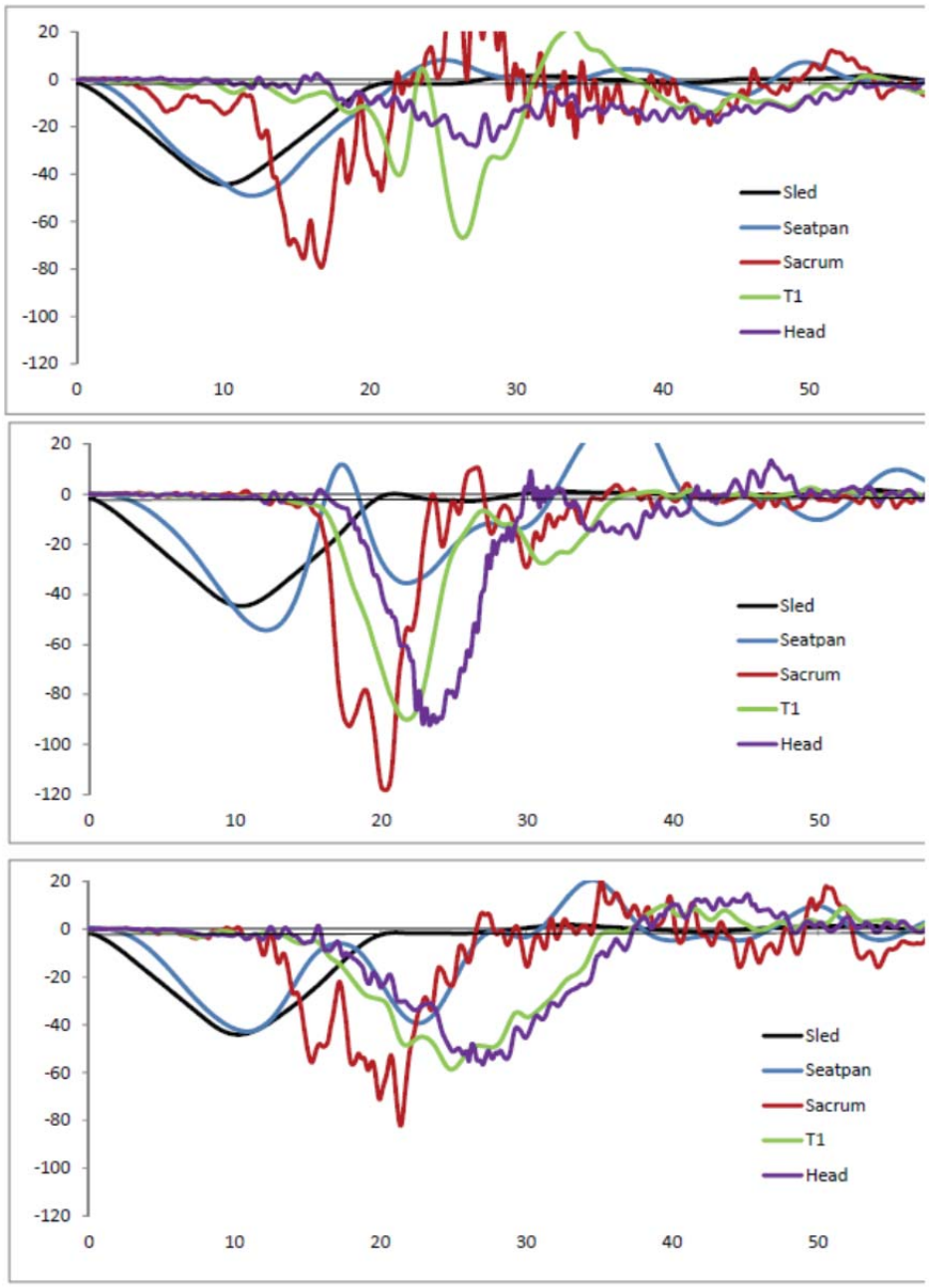

For the three plots above, the top is for a PMHS, the middle is for a Hybrid-III dummy with curved lumbar spine, and the bottom is for a SID-HIII dummy with a straight lumbar spine. The vertical axis is acceleration in G's and the horizontal axis is time in msec. The test with the PMHS resulted in a pelvic ring fracture.

The relative timing of when the particular body part accelerates due to under-seat acceleration may be a good biofidelity criterion for an advanced dummy that is used to assess under-body blasts. Below are preliminary plots for the ten test conditions comparing the relative timing of seat (sled), pelvis, thoracic spine, and head for the two dummies compared to PMHS.

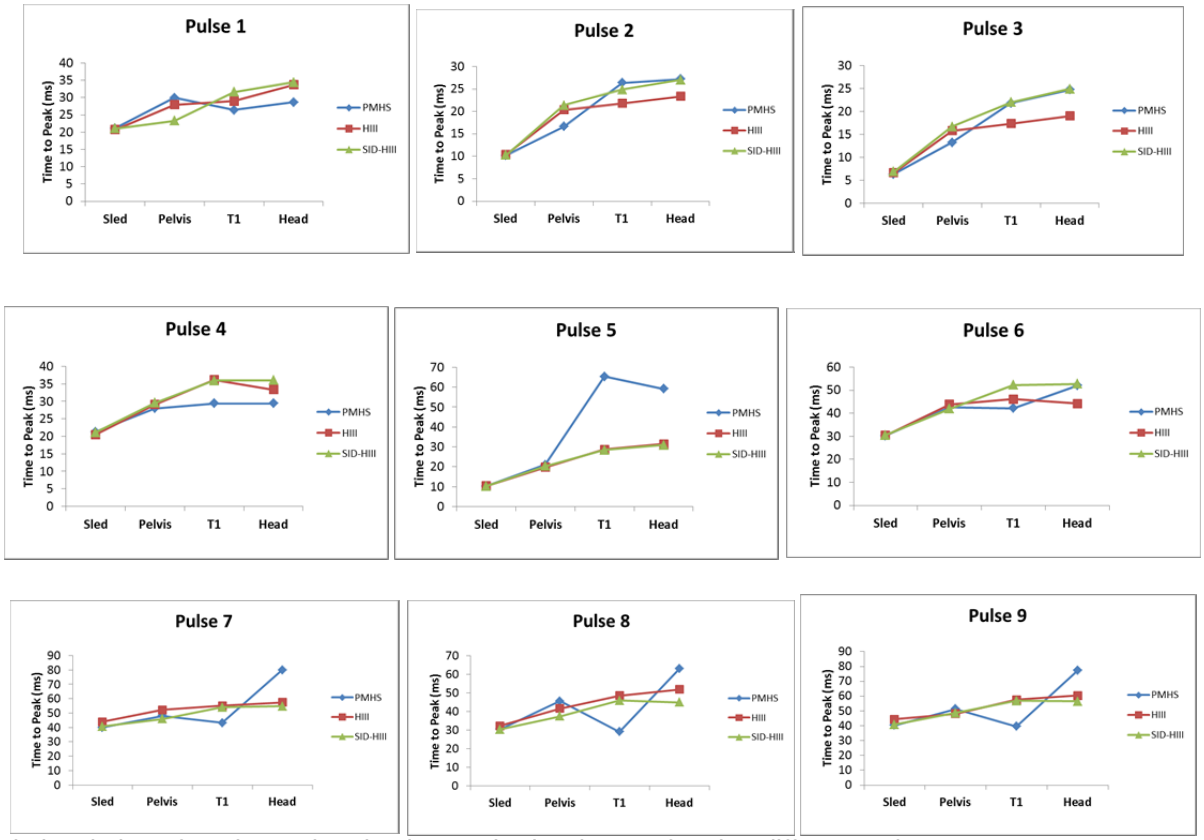

Relative timing of peak acceleration in matched-Pair tests for nine different pulses.

In many of the test conditions the time to peak for body segments further away from the pulse is longer for PMHS than for dummy. This would imply a greater decoupling of body segments in the human.

Tests with Army THOR dummy: 32 sled tests were conducted with a THOR dummy according to protocols described in previous reports. The dummy was instrumented with a five-axis load cell above the lumbar flex-joint, along with accelerometer and neck load cell locations comparable to the Hybrid-III dummy. The results from the THOR test series can be compared with HIII data both in the normal and straight-spine configurations, as THOR has a straighter lumbar region, but also a different pelvic tilt. Another PMHS test series was also conducted, with a sigmoidal-shaped input acceleration pulse. The specimen was tested in a slouched position to allow for straightened alignment of the lumbar spine region. The series resulted in a burst fracture at the L1 level, with no other fractures present in the lumbar or pelvic components.

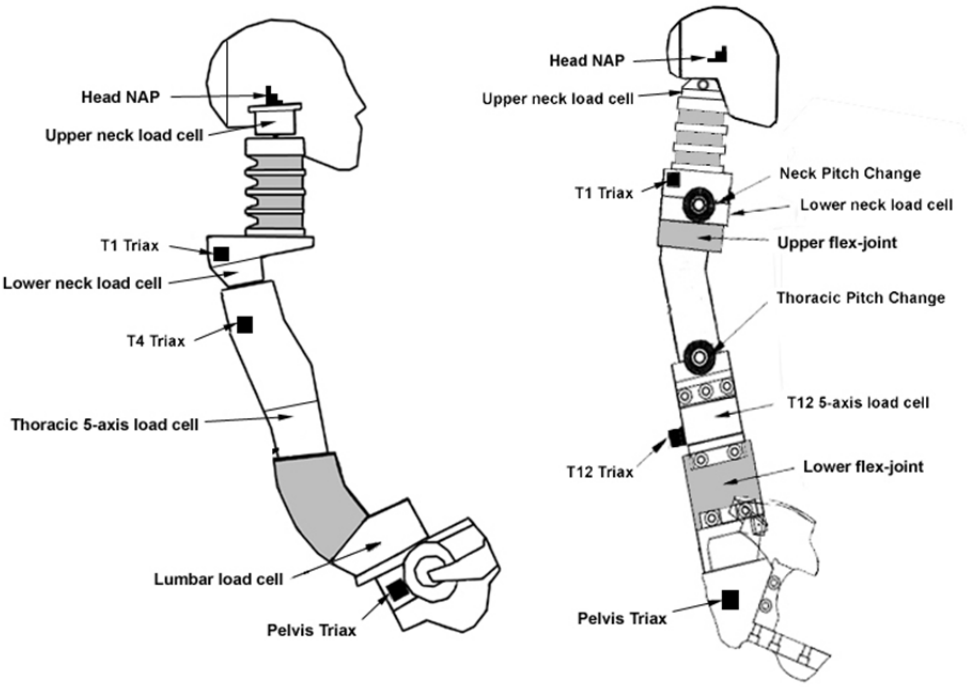

Comparison of THOR (right) dummy instrumentation locations vs. HIII (left) with thorax and lumbar load cells.

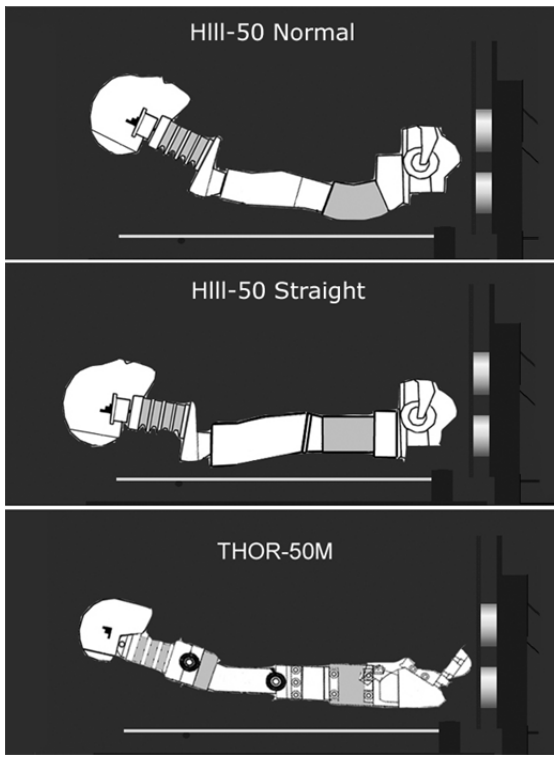

Three different dummy spine configurations in the tested positions.

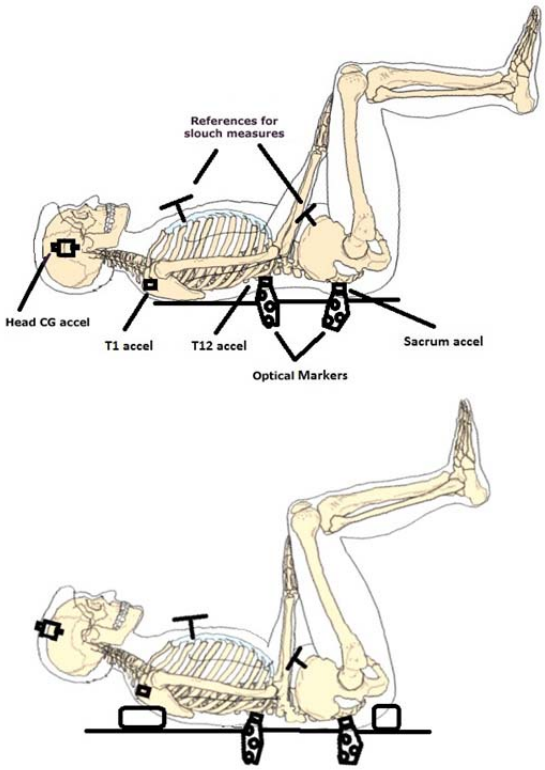

Normal (top) and slouched (bottom) positioning of the PMHS to allow for straightened lumbar alignment.

Below is a typical dataset from surrogate instrumentation in two matched-pair test series. The first figure demonstrates two sled acceleration traces that have matched pair results for the THOR, HIII in the straight and curved spine configuration with lumbar load cells, and a PMHS. The next figure shows acceleration trace comparisons for these tests, from the head to the pelvis for both Hybrid III configurations, the THOR dummy, and a PMHS. The ATD surrogates are also compared in these tests for loading along the neck and spine. All tests were conducted with a 2" honeycomb padding on the seat pan to avoid buttocks flesh deterioration. The forces in the ATD generally follow the acceleration input, with the THOR showing some significant differences in magnitude from the HIII.

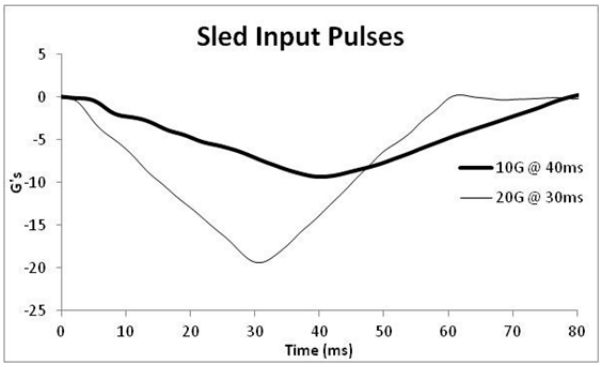

Two sled pulses of varying magnitude and width under which a HIII has been tested in two different configurations, as well as a THOR and a PMHS.

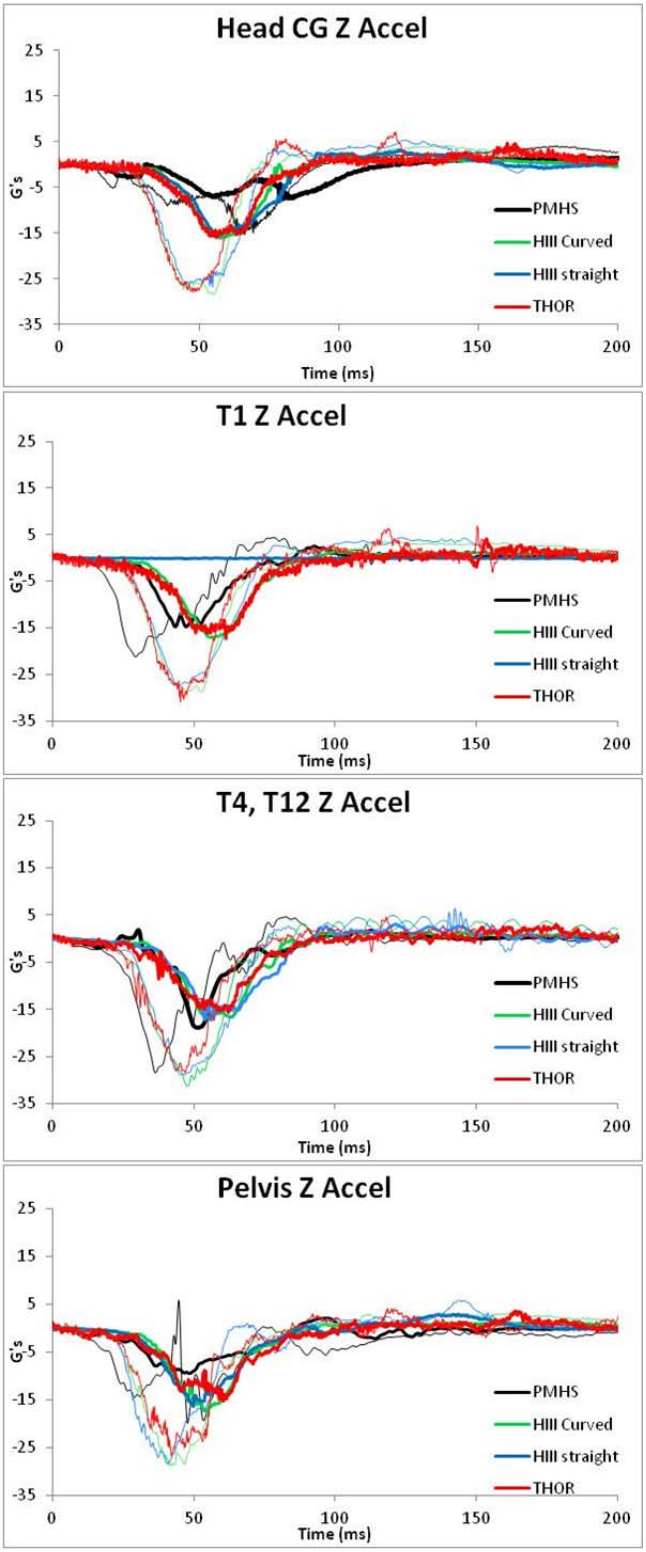

Acceleration traces for a matched-pair test series from the pulses shown above. Thick lines are for the 10G pulse, thin lines for the 20G. Note: T1-Z channel failed in the HIII straight-spine test. T4 acceleration data for the HIII is compared to T12 data in the THOR since T4-12 is rigidized in the HIII.

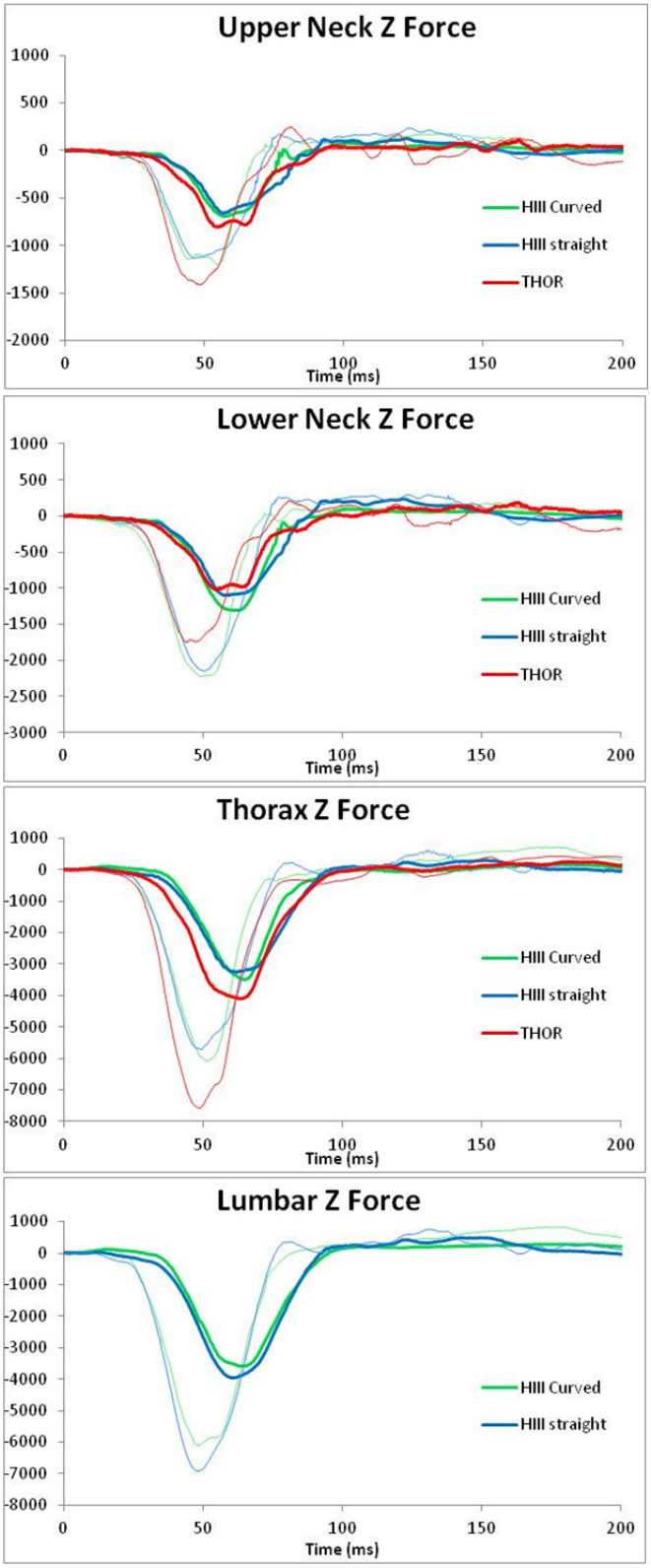

ATD loads along the spine for the same pulses presented in above. Thick lines are for the 10G pulse, thin lines for the 20G. Note: THOR not equipped with a lumbar load cell.

The most recent PMHS testing was administered with a sigmoid shaped pulse to allow for slower initial onset loading before reaching peak magnitude and speed. This was done to explore the effect of a cushioned seat or an energy absorbing seat. The goal was to produce a lumbar spine fracture without a pelvis fracture. The pulses were of longer duration than previous tests, and the peak accelerations increased for each succesive test within the four-test series. Figure 7 shows the four pulses for this PMHS series.

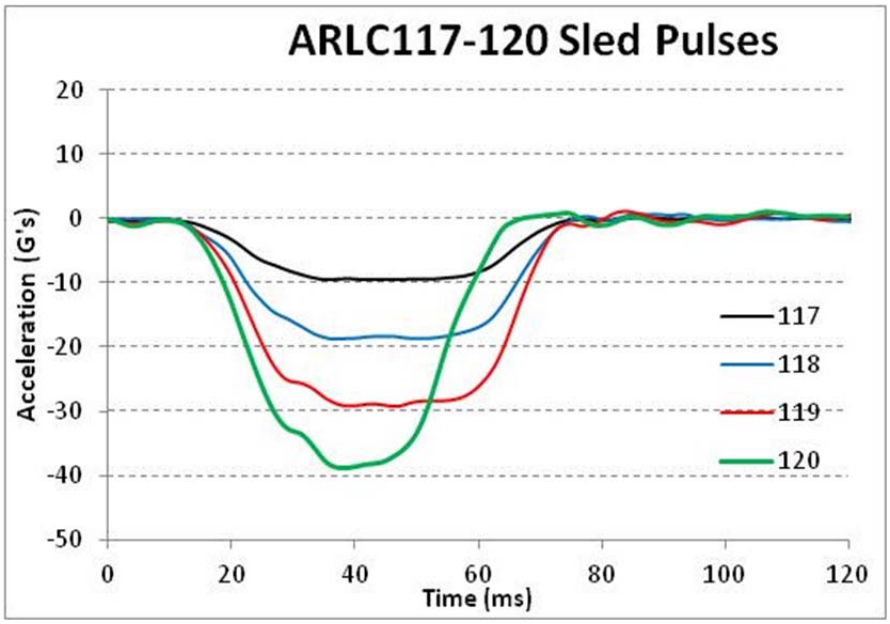

The four pulses for the last PMHS test series.

Although the input pulse peaks occurred at relatively the same time, as they were targeted as such, the resulting acceleration peaks in the lumbosacral region varied. The higher the magnitude of the input pulse, the wider the time-variation between T12 and sacrum peak acceleration for this test series. The sigmoidal pulse seems to induce a two-phase loading of the lumbar-pelvic complex, where the lower region absorbs energy during an onset phase, before the upper region is loaded during the more intense part of the pulse. The alignment of the lower vertebra and pelvic tilt likely contribute to the ability of the lower region to absorb the initial shock. Given the unique pulse and injury patterns seen for this PMHS, further insight into the relationship between onset rate and level of injury is needed.

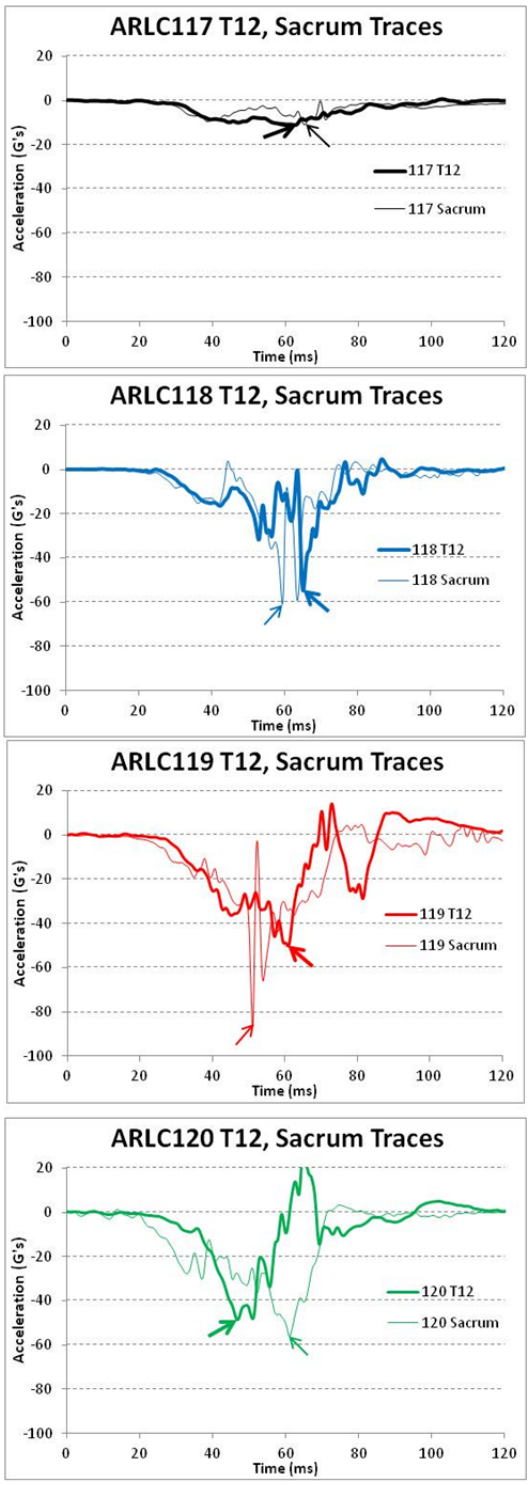

Time traces of T12 and sacrum accelerations for the latest PMHS. Arrows indicate peaks and show an increasing time-gap with greater magnitude input pulse.

In many of the test conditions the time to peak for body segments further away from the pulse is longer for PMHS than for dummy. This would imply a greater decoupling of body segments in the human.

Summary of PMHS Testing:
Exploratory tests have been conducted to determine the mechanism of lumbar spine fracture due to vertical (Gz) seat pan loading. The goal of the testing was to determine what pulse shape characteristics at high loading rates representative of the underbody blast loading environment are unique to either pelvic fracture or lumbar spine fracture. 20 Sled tests have been conducted on 5 different full-body post-mortem human surrogates (PMHS, or cadaver), with input pulse characteristics varying in peak G level, jerk, and delta-V. Each specimen underwent pulses of increasing intensity until injury was recognized, except for specimen 3, which was tested to just below what was believed to be the injury threshold. Table 1 gives general specimen information.

PMHS	Height (cm)	Weight (Kg)	Sex	Age (yrs)
1	185	67	M	57
2	182	75	M	58
3	177	58	M	63
4	176	61	M	84
5	172	61	M	54

Table 1. General specimen information.

To summarize the approach for each specimen:
PMHS-1: Unpadded testing under ramp input pulses. Two initial identical low jerk pulses to observe repeatability between tests, followed by two sharper pulses, the last one causing extensive injury to pelvic components.
PMHS-2: Same approach as specimen one, except using 2" cardboard honeycomb padding at the seat interface. Two low grade pulses followed by a medium grade before injuries were recognized at the right side sacroiliac joint and pubic ramus.
PMHS-3: Wider pulse widths and lower jerk investigated. Five tests of increasing intensity, with the last two at higher speeds than any tests so far. Last test was done with specimen orientated to achieve straight lumbar spine alignment. No fractures were found in thoracic, lumbar, or pelvic regions.
PMHS-4: Pulse morphology changed from triangular to sigmoidal, straight lumbar alignment for each test. Pelvic injury locations were similar to earlier tests, bilateral and not as severe. First indication of upper lumbar injury with compression fracture at T12 indicated on CT scan.
PMHS-5: Four sigmoidal pulses of longer duration than PMHS 4 and increasingly higher peaks. Straight lumbar spine alignment. No pelvic fractures, but isolated L1 burst fracture.

Test Setup

Specimen Instrumentation: Specimens were instrumented by experienced personnel who fixated accelerometer and optical marker mounts to specifically targeted anatomical landmarks. Tri-axial accelerometer blocks were placed in line with approximated head center of gravity, on the posterior T1 and T12 vertebral bodies, and at the mid-sacral plate. Mounts for the optical tracking system were also mounted at T12 and the sacrum, and on the both iliac crests for specimens four and five. The iliac crest was also used as a reference to measure the degree of 'slouch' instituted between tests. Small aluminum plates were affixed tangentially at the sternum and right anterior superior iliac spine. The difference between these angles when the specimen was laying flat and in the tested position was defined as the degree of slouch. The coordinate system was adapted from the SAE J211.

Sled Buck: Input pulses were programmed into an acceleration sled at varying peaks and onset levels. A steel buck was constructed to accommodate biological variations such as femur

and shin length, and to administer test conditions such as seat back angle and seat contact area. A slot in the seat back was created to allow for clearance of markers that tracked motion of T12 and the sacrum. The seat pan was instrumented with four tri-axial load cells and the footpan with two.

Specimen Alignment: For most tests, the specimen-seat interface was padded with two inches of honeycomb cardboard rated at 30 psi. A lap belt was placed just inferior to the iliac crest and bilaterally across each acetabulum to restrain the pelvis upon rebound from the contact with the seat pan. Similar control was achieved with loose head and torso belt restraints. All restraints aimed at avoidance of flailing while preventing interference with the dynamics of compression. The arms were secured to avoid any interference with external markers. For alignment, the torso was laid flat on the seat back for about half the tests and for the others the specimen was flexed into a slouch position to straighten the lumbar spine. This was done with 6" of padding beneath the scapula and 2" beneath the ischial tuberosities to tilt the pelvis and torso toward each other. The result was between 25 and 40 degrees of slouch for these tests compared to the flat 0 degree supine tests.

Data Acquistion: Data was acquired at 20 kHz sampling rate via an onboard TDAS. High speed video cameras were positioned overhead, right laterally, and onboard underneath the seat. A 1 kHz 20-camera retro-reflective 3D motion capture system was used to track motion targets at of the sled, torso, T12, and pelvis.

Results

Overall injury results are provided for the five PMHS, however three of the five tests resulting in injury are highlighted. A more detailed report with electronic data will be provided as part of the project deliverables. The three highlighted tests demonstrate a test condition that resulted in pelvis fractures alone, another test condition that resulted in pelvis and a minor lumbar spine fracture, and a third test condition that resulted in a lumbar spine fracture with no pelvis fractures.

Injuries: A complete autopsy was performed on each specimen by a certified pathologist. Table 2 summarizes the results for each of the specimens tested.

Table Autopsy results for the five specimens tested.

Pulse #	**TESTID**	**PMHS**	**Injuries**
1	ARLC101	1	BILATERAL SACROILIAC PELVIC FRACTURES: Complete dislocation. LEFT PUBIC CREST: Partial. LEFT PUBIC RAMUS fracture. L5 VERTEBRAL BODY SPINOUS PROCESS fracture.
1	ARLC102	1	
2	ARLC103	1	
3	ARLC104	1	
1	ARLC105	1	
1	ARLC106	2	RIGHT SACROILIAC (COMPLETE SEPARATION) RIGHT PUBIC CREST (SUPERIOR PUBIC RAMUS) RIGHT ISCHIUM (INFERIOR PUBIC RAMUS) LEFT ILIUM (ILIAC FOSSA)
1	ARLC107	2	
2	ARLC108	2	
4	ARLC109	3	Thoracic and lumbar spines were not fractured; no abnormal curvature or osteophytes were noted. The sacrum and pelvis were not fractured.
5	ARLC110	3	
6	ARLC111	3	
7	ARLC112	3	
8	ARLC113	3	
9	ARLC114	4	BILATERAL SACROILIAC PELVIC FRACTURES: Complete separation of the sacrum and iliac bones in a vertical pattern bilaterally. SACRUM:
10	ARLC115	4	

11	ARLC116	4	Fractured through hardware mounts with a complete horizontal fracture. COCCYX fractured. T12 compression fracture by CT.
12	ARLC117	5	L1 VERTEBRAL BODY AND LAMINA BURST FRACTURE. No pelvic fractures. Small coccyx fracture with no dislocation.
13	ARLC118	5	
14	ARLC119	5	
15	ARLC120	5	

Post-test radiology for PMHS-2, PMHS-4, and PMHS-5

Left: 3D radiology image demonstrating pelvic fractures; Middle: 2D Sagittal plane CT demonstrating minor T12 fracture; Right: CT image demonstrating L1 burst fracture.

Highlighting the difference between various sled pulses and their effect, the following plots demonstrate the difference in loads and accelerations to various body regions for the three PMHS with different injuries as shown in Figure 2. It appears that the sharp onset pulse creates pelvic fractures, while the sigmoid-shaped drawn-out pulse produces lumbar spine fractures.

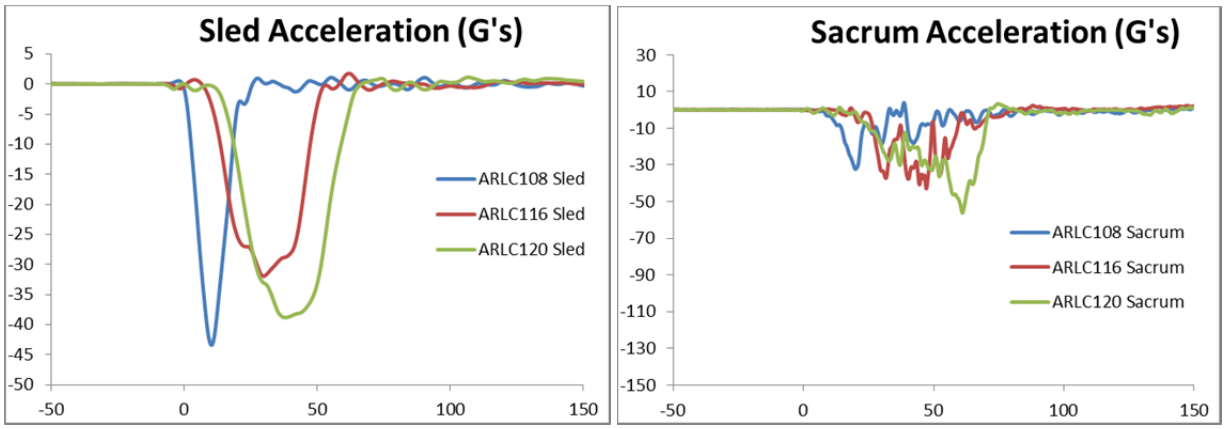

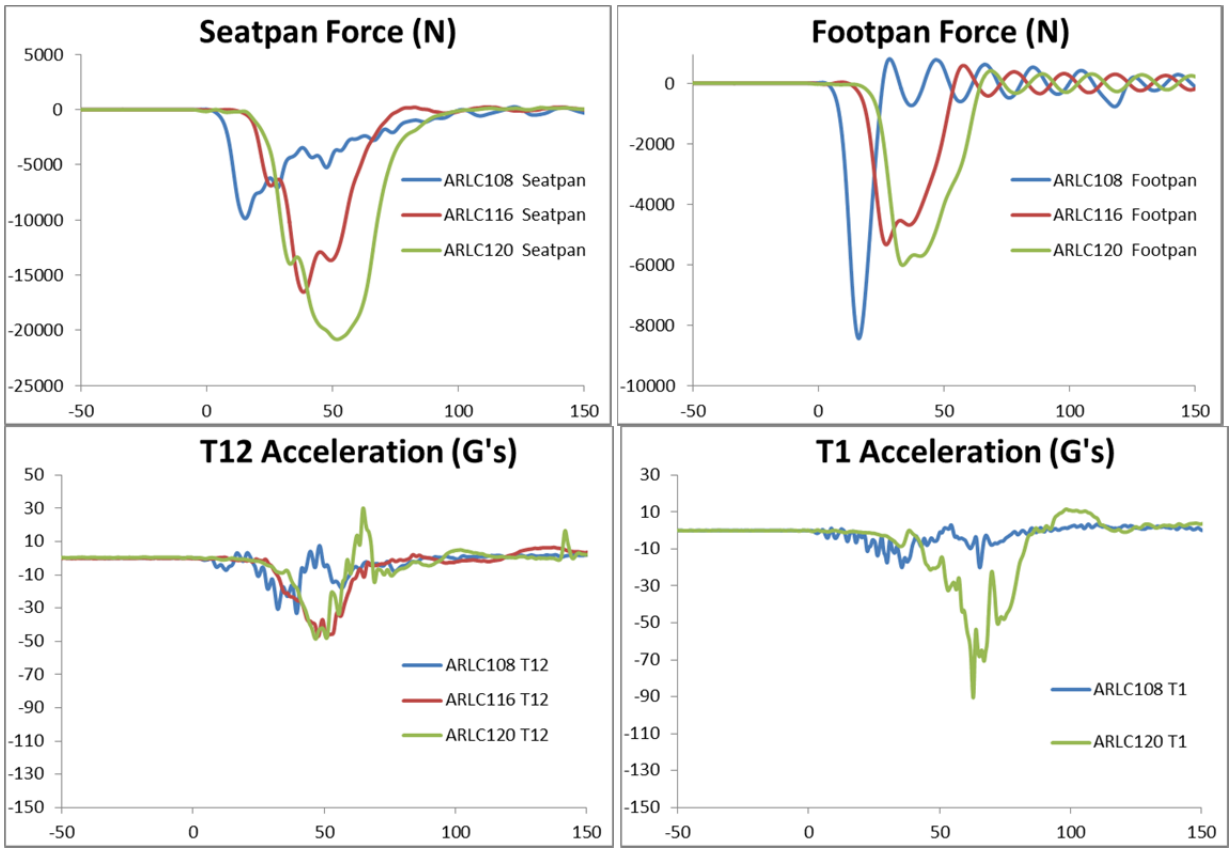

TASK 3: CERVICAL SPINE FINITE ELEMENT MODEL

MCW Cervical Spine Finite Element Model

GESAC received a copy of the Abaqus finite element model of the human cervical spine developed by MCW. The model represents the spine structure between C4 – C7, including associated ligaments. The goal of the initial work was to translate the Abaqus to LS-DYNA model.

Frontal flexion deformation of LS-DYNA C4-C7 model (moment = 0 Nm; 1 Nm; 2 Nm)

Testing of LS-DYNA Model

Summary of Comparison of Abaqus and LS-DYNA Models: The LS-DYNA model consists of the following:

Geometry: Identical to Abaqus model

Materials:

I. simple elastic materials in Abaqus remained simple elastic (e.g. cortical and cancellous bones)
II. non-linear elastic (hyperfoam in Abaqus) was initially modeled as elastic with the Young's modulus estimated from the linear approximation of the Abaqus model (e.g. disc components)
III. elastic membranes remained elastic membranes (e.g. components of the synovial facet joints and Luschka's joints)
IV. fluid materials in Abaqus were initially modeled as elastic materials with Young's modulus and Poisson's ratio estimated from the water bulk modulus (enclosing membranes of the synovial fluid and Luschka's joint)
V. all ligaments were modeled as discrete springs with the force-deflection function identical to the Abaqus definition.

Boundary Constraints: All inferior nodes of the C7 vertebra (part C7TUBERCLE) were fully constrained. Nodes at the superior edges of the top plate (part PLATE) were constrained for specific degrees of freedom, depending on the loading condition.

Loading Condition:

I) for flexion, loads were applied to the individual nodes of the superior edges of the PLATE part at both the anterior and posterior ends; loads were directed in the +X direction at the anterior edge and –X direction at the posterior edge; maximum loads of 1.12N were applied at each node, and with a total of 23 nodes at each edge resulted in a total moment of 2Nm as specified in the Abaqus model.
   a. for extension, the loading was identical to flexion, except loads were in the –X direction at the anterior edge, and +X direction at the posterior edge.
   b. for lateral flexion, the loading was applied at all the nodes of the superior right and left edges of the PLATE part; loads of 2.44N were applied at each of the 20 nodes at each side, resulting in an effective moment of 2Nm; the direction of loading at the right edge was in the +X direction and at the left edge in the –X direction.
   c. for axial rotation, the loading was applied at all the nodes of the superior anterior and posterior edges of the PLATE part; loads of 1.12N were applied at each node resulting in an effective axial moment of 2Nm; the direction of loading at the anterior edge was in the +Z direction and at the posterior edge is in the –Z direction.
   d. for all loadings, the time to reach maximum loading was set to 0.80 sec and the model was run for another 0.20 msec (total simulation time 1.00 msec) to ensure stability.

What follows is a description of the LS-DYNA model simulations that have now generated a validated baseline intact model. Each loading mode is outlined below.

Extension

The model was significantly out of corridor, in the extension load case. Attempts were made to stiffen the ALL which brought it closer to the corridor, however, not within the corridor entirely. The ALL was also near its functional limit of affecting the model response. The facet joint modifications were also insufficient in and of themselves to bring the model into corridor. The facets also have more of an effect on the model in the other loading directions and can push the model out of corridor relatively quickly. Earlier attempts at modifying both the ALL and facet together in a model run failed convergence in implicit. Neither the ALL nor the Facet were sufficient alone to bring the model response within corridor. Previous attempts at running the model with ALL and Facet modifications resulted in convergence failures. It was decided to modify the annulus in conjunction with the ALL. The following models have the modification of stiffening the ALL (6x) and stiffening the Posterior and Anterior Annulus (10x). The results are as follows. The model successfully ran to full load and convergence at equilibrium with ALL 6x and Annulus 10x. Modifying the annulus instead of the facet gives better overall results for model response. Note that for C45 the response is largely within corridor for the majority of the load application. The response however does exceed the upper corridor somewhat during the last portion of the load application. Also note that the trajectory is linear which may be a contributing factor in pushing the model out of corridor.

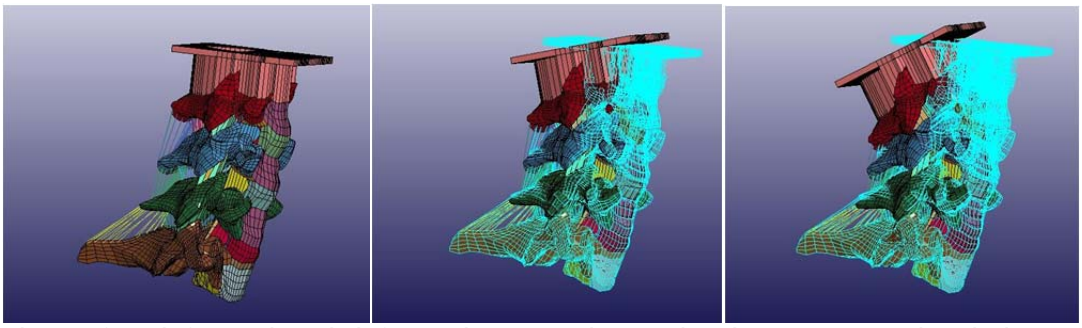

Comparison of undeformed and deformed geometries at the three moment levels in extension (moment = 0 Nm; 1 Nm; 2 Nm).

Flexion

The model was run in Flexion after the Anterior Longitudinal Ligament was multiplied by 6.0 and the Posterior and Anterior Annulus parts were multiplied by 10.0. All other material properties were held constant. The model ran to completion while taking the full load and the solution converged fully at the full load and maintained equilibrium. The results are as shown below. The response for the model in flexion shows C45 primarily within corridor. The responses for C56 and C67, however, are slightly out of corridor and very closely follow the lower bound of the corridor for both cases. Since the ALL plays no role in flexion, it can be seen that the annulus (stiffening 10x) is driving the model out of the lower bound corridor in the C56 and C67 segments. Softening the annulus will pull the model back in corridor in Flexion. However, as indicated above, extension is still out of corridor (high) for C45, as such the softening of the annulus will push this further out of corridor. A potential solution is to soften the annulus while

stiffening the ALL, which may improve flexion and extension simultaneously. This is currently being reviewed.

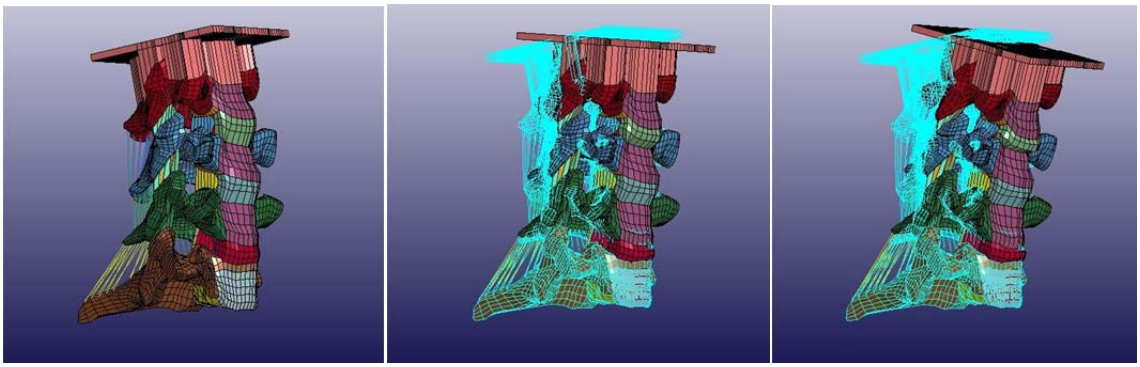

Comparison of undeformed and deformed geometries at the three moment levels in frontal flexion (moment = 0 Nm; 1 Nm; 2 Nm).

Lateral Bending

The model was run in Lateral after the Anterior Longitudinal Ligament was multiplied by 6.0 and the Posterior and Anterior Annulus parts were multiplied by 10.0. All other material properties were held constant. The model ran to completion while taking the full load and the solution converged fully at the full load and maintained equilibrium. The results are as shown below. The model is within corridor at the peak load for C56 and C67 but still a bit low for the C45 segment. The softening of the annulus as described in section A.3 above may improve the response in lateral.

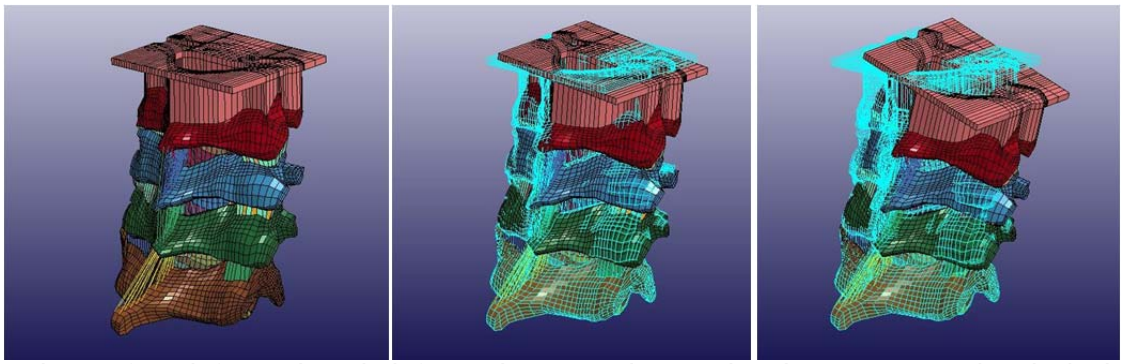

Comparison of undeformed and deformed geometries at the three moment levels in lateral flexion (moment = 0 Nm; 1 Nm; 2 Nm).

Axial Torsion

The model was run in axial after the Anterior Longitudinal Ligament was multiplied by 6.0 and the Posterior and Anterior Annulus parts were multiplied by 10.0. All other material properties were held constant. The model ran to completion while taking the full load and the solution converged fully at the full load and maintained equilibrium. The results are as shown below. The axial load case responses for C45 and C56 fall within corridor for ½ the load application and C45 is in corridor at the peak load with C56 slightly out of corridor (high) at peak load. The C67 segment however diverges above the corridor more. Note that the irregularities in the curves seem to correspond to large element deformations resulting in poor element quality in

the facet joint region. Note that the improved axial response is due to the correction of an erroneous boundary condition which was applied to the model. An initial review of the model shows high deformation in the area of the facet joints.

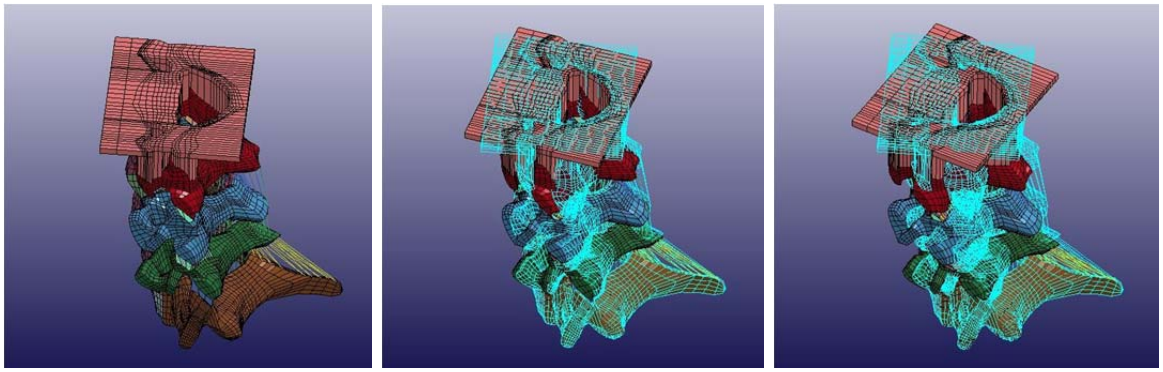

Comparison of undeformed and deformed geometries at the three moment levels in axial rotation (moment = 0 Nm; 1 Nm; 2 Nm).

Results and Discussion

Combinations of a further stiffened ALL (8x) and Annulus (10x) gave better results within the corridor for extension and brought the curve almost entirely within corridor. Cleaning up the model with the Model Shakedown" procedure resulted in a significant reduction in the number of runs failing due to convergence failures and negative element volumes. New plots shown below demonstrate that the model is at worst 85% in the corridor and at best 100% in the corridor. Comparison is made between the old model by Shams (red), the published MCW model by Wheeldon (light blue) and the most recent effort (dark blue). The model is now considered validated for the present effort, and obtaining internal parameters of stress, strain, and load sharing with fusion and ADR models will be forthcoming.

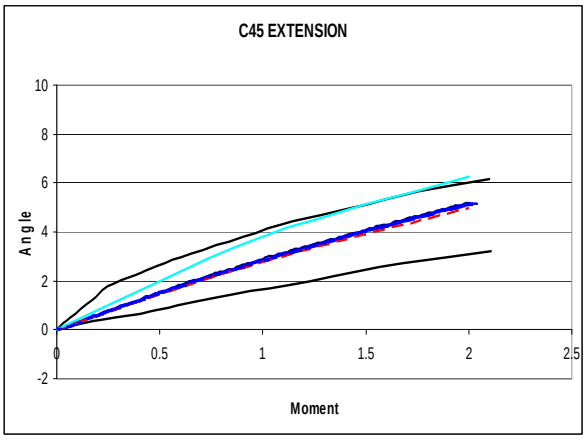

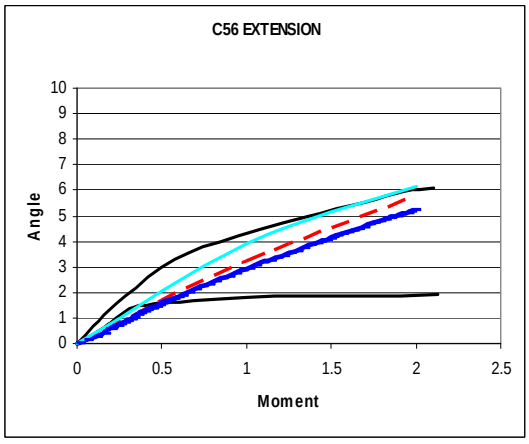

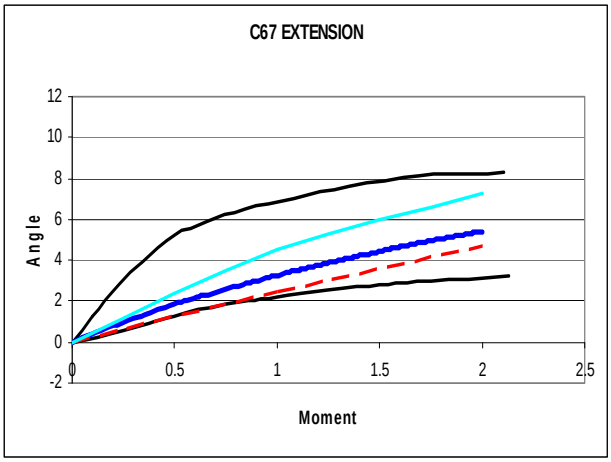
C67 EXTENSION
Angle
Moment
12
10
8
6
4
2
0
-2
0
0.5
1
1.5
2
2.5

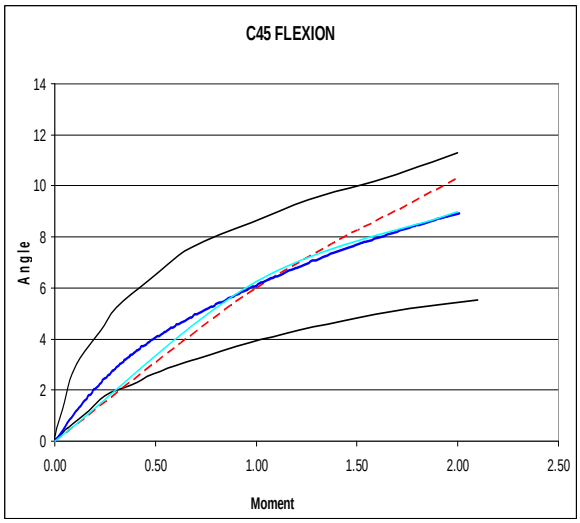
C45 FLEXION
Angle
Moment
14
12
10
8
6
4
2
0
0.00
0.50
1.00
1.50
2.00
2.50

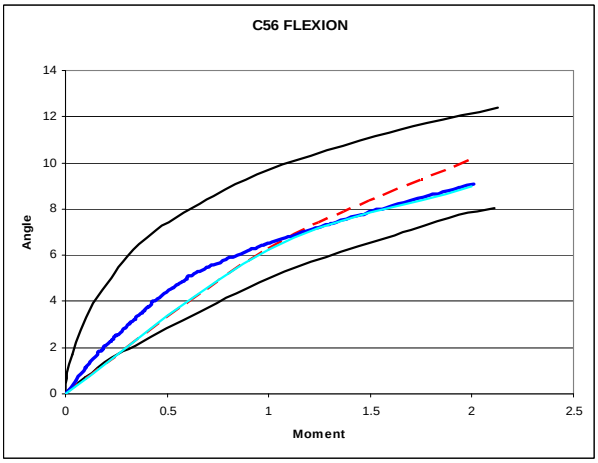
C56 FLEXION
Angle
Moment
14
12
10
8
6
4
2
0
0
0.5
1
1.5
2
2.5

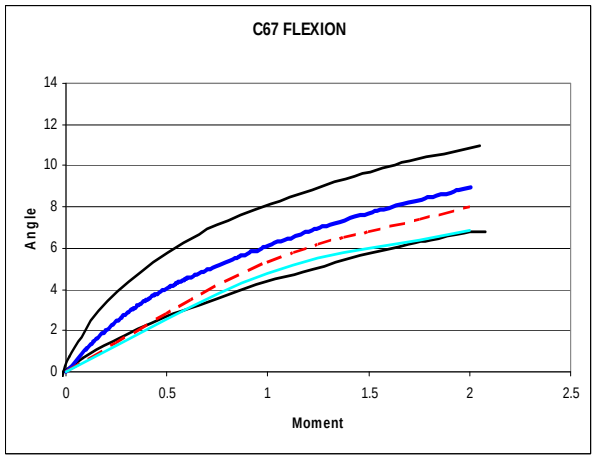
C67 FLEXION
Angle
Moment
14
12
10
8
6
4
2
0
0
0.5
1
1.5
2
2.5

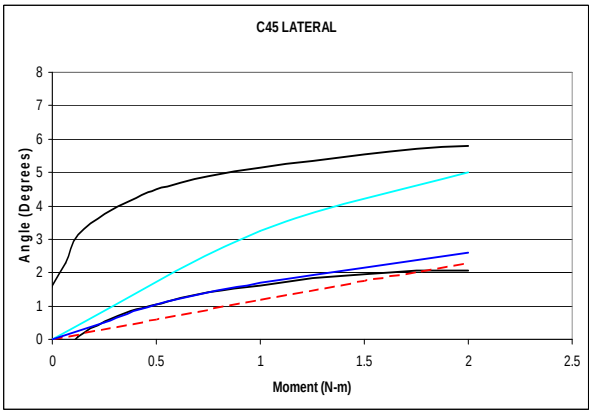
C45 LATERAL
Angle (Degrees)
Moment (N-m)
8
7
6
5
4
3
2
1
0
0
0.5
1
1.5
2
2.5

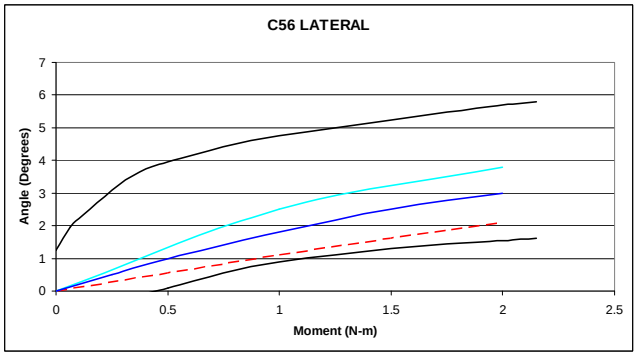
C56 LATERAL
Angle (Degrees)
Moment (N-m)
7
6
5
4
3
2
1
0
0
0.5
1
1.5
2
2.5

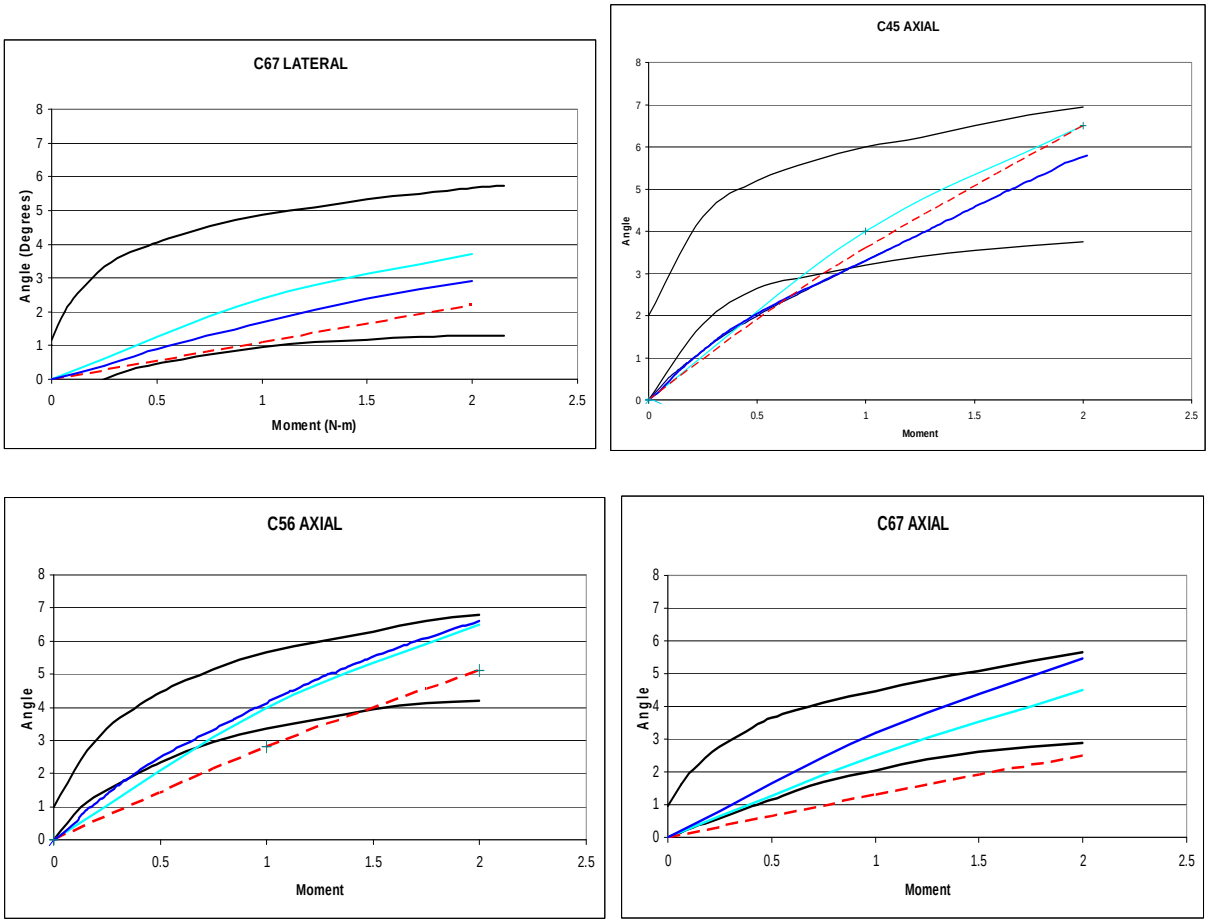

TASK 4 IN VIVO CERVICAL ARTIFICIAL DISCS IN ANIMAL MODEL

Review of CDR and *in vivo* Biomechanics

Based on the clinical review of ADR and biomechanical studies on the topic, two artificial discs were selected to conduct longitudinal studies with the Caprine model. Bryan and Pro-disc were selected. The animals that had the first Bryan disc implants had three-month x-rays to document progress. It was determined that in two of the animals, the artificial disc had protruded out of the disc space and was causing discomfort to the animal. These two animals were sacrificed based upon the recommendation of the veterinarian and concurrence of the surgeon and PI. The first animals coming off study were sacrificed in January and February. A second series of animals were done with implants at one spinal level down to see if spinal level consistency would improve outcome. A biomechanical testing protocol is being evaluated in trial specimens until more spines from the animals are collected. The testing protocol includes quasi-static testing so that comparisons to previous studies can be made, but will also include non-destructive and destructive dynamic testing that is meant to mimic the harsher loading in the military environment. Testing will apply dynamic loads to the superior spine segments to mimic an approximate five-G loading environment to the head.

Artificial Cervical Disc and *in vivo* Biomechanics

Based on the clinical review of ADR and biomechanical studies on the topic, two artificial discs were selected to conduct longitudinal studies with the Caprine model. Bryan and Pro-disc were selected. A

total number of 21 goats have undergone an anterior cervical discectomy. In the past three months another five goats have undergone Pro-Disc-C ADR surgery at the C3-C4 level because of the relatively poor outcome of the goats done at the C2-3 level and to match the goats that had surgery at that same level with fusion and Bryan-Disc ADR. At the end of their survival time, the animals were euthanized; the five most recent animals have been surviving for 3-months already. Of significance, this study appears to be the only animal investigation that will have head-to-head comparisons of two implants from two different companies. For this reason the companies have not been very cooperative and are charging our research the full retail cost of the implants.

Animal ID	Procedure	Surgery Date	3-Month Xray	Euthanize	Evaluation
CDRG100	Bryan	12-Jul-11	18-Oct-11	17-Jan-12	Excellent placement, no migration or osteolysis
CDRG200	Bryan	19-Jul-11	18-Oct-11	17-Jan-12	Excellent placement, no migration, thin rim of hypodensity between inferior endplate of C2 and the device at 3 months that is much less apparent at 6 months
CDRG300	Bryan	21-Jul-11	18-Oct-11	25-Oct-11	Extrusion at 3 months, intraoperative images show well placed device, vertebral endplates may have been drilled excessively
CDRG400	Bryan	21-Jul-11	18-Oct-11	25-Oct-11	Extrusion at 3 months, intraoperative images show well placed device, vertebral endplates may have been drilled excessively
CDRG500	Bryan	21-Jul-11	18-Oct-11	24-Jan-12	Excellent placement, no migration or osteolysis
CDRG600	Fusion	26-Jul-11	18-Oct-11	24-Jan-12	C2 screws pulled out 60% at 3 months, stable at 6 months, evidence of bony fusion
CDRG700	Fusion	26-Jul-11	18-Oct-11	24-Jan-12	Excellent placement of hardware, evidence of bony fusion, no hardware migration
CDRG800	Fusion	9-Aug-11	18-Oct-11	31-Jan-12	Excellent placement of hardware, evidence of partial bony fusion, no hardware migration
CDRG900	Fusion	16-Aug-11	16-Nov-11	14-Feb-12	Excellent placement of hardware, evidence of bony fusion, no hardware migration
CDRG1000	Fusion	23-Aug-11	16-Nov-11	14-Feb-12	Excellent placement of hardware, evidence of partial bony fusion, no hardware migration
CDRG1100	ProC	18-Aug-11	16-Nov-11	14-Feb-12	Excellent placement, no migration, thin rim of hypodensity along superior and inferior keel/endplate of device
CDRG1200	ProC	18-Aug-11	16-Nov-11	21-Feb-12	Excellent placement, no migration, thin rim of hypodensity along superior and inferior keel/endplate of device
CDRG1300	ProC	23-Aug-11	16-Nov-11	21-Feb-12	Excellent placement, no migration or osteolysis
CDRG1400	ProC	25-Aug-11	16-Nov-11	28-Feb-12	Excellent placement, no migration, thin rim of hypodensity along superior and inferior keel/endplate of device noted at 3 month, not at 6 months
CDRG1500	Fusion	25-Aug-11	16-Nov-11	28-Feb-12	Excellent placement of hardware, evidence of partial bony fusion, no hardware migration
CDRG1600	ProC	25-Aug-11	16-Nov-11	28-Feb-12	Device partially extruded (30%) at 3 months, stable at 6 months, superior endplate of C4 may have been excessively drilled intraoperatively
CDRG1700	Control				
CDRG1800	Control				
CDRG1900	Bryan	1-May-12			

CDRG2000	Bryan	1-May-12			
CDRG2100	Bryan	1-May-12			
CDRG2200	Bryan	3-May-12			
CDRG2300	Bryan	3-May-12			

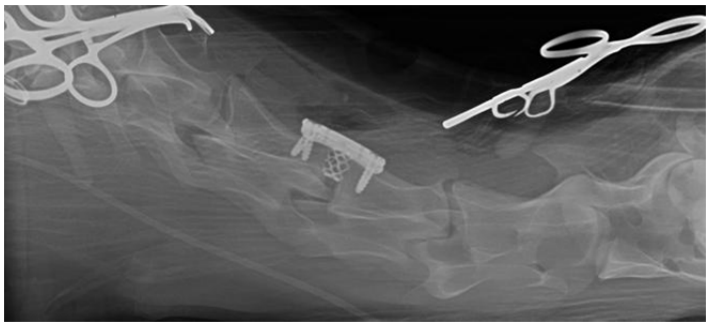

Radiograph of goat cervical spine demonstrating anterior cervical discectomy and fusion.

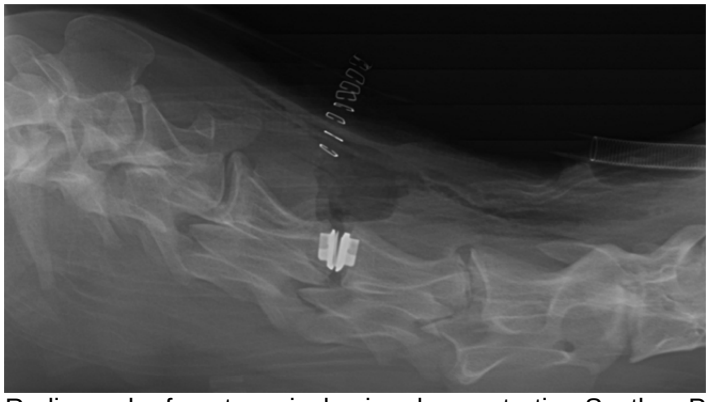

Radiograph of goat cervical spine demonstrating Synthes Pro-C artificial disc.

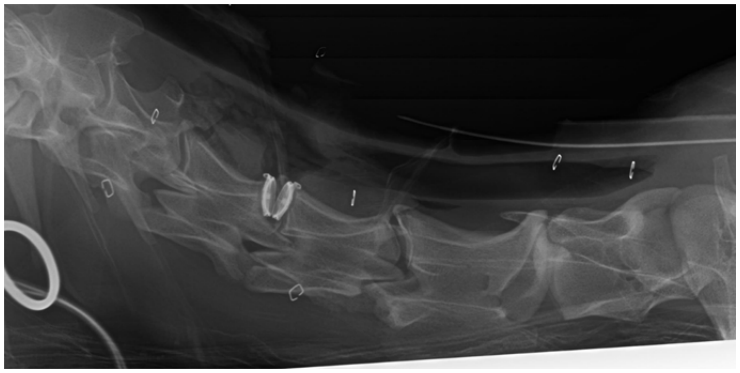

Radiograph of goat cervical spine demonstrating Medtronics Bryan artificial disc.

Upon sacrifice, the cervical spine of each animal was harvested and placed in a freezer to await biomechanical testing. A testing protocol for the biomechanics portion of this study has been is outlined below and preliminary testing has begun. Because the caprine ligamentous cervical spine is quite flexible, initial use of an apparatus used with human cadaver spines applied too great of an initial bending load to the specimen preparation. The apparatus has been redesigned for goat spine testing and experimental testing has been resumed.

Caprine Cervical Spine Biomechanical Testing Protocol

Specimen Preparation:
- Pre X-rays
- Clean / Pot Specimens
- Instrument Specimen
- ± 100G accelerometer on superior potting

Test Preparation:
- Piston Air Runs
- Equipment Set-up
- Place Instrumentation for Piston
- Uniaxial Load Cell Superior to Specimen
- 6-Axis Load Cell Inferior to Specimen

Testing:

Quasi – Static Combined Loading
- Lateral Bending / Compression
  Displacement = 2.5cm ; Moment Arm Eccentricity = 4cm ; Rate = 1cm/s
- Flexion / Compression
  Displacement = 2.5cm ; Moment Arm Eccentricity = 4cm ; Rate = 1cm/s
- Extension / Compression
  Displacement = 2.5cm ; Moment Arm Eccentricity = 4cm ; Rate = 1cm/s
- Axial Rotation / Compression
  Displacement = 2.5cm (Rate = 1cm/s) ; Rotation = 30°

Dynamic Combined Loading
- Lateral Bending / Compression
  Displacement = 2.5cm ; Moment Arm Eccentricity = 4cm ; Rate = 50cm/s
- Flexion / Compression
  Displacement = 2.5cm ; Moment Arm Eccentricity = 4cm ; Rate = 50cm/s
- Extension / Compression
  Displacement = 2.5cm ; Moment Arm Eccentricity = 4cm ; Rate = 50cm/s

Specimen Failure
- Flexion / Compression
  Displacement = 20cm ; Moment Arm Eccentricity = 4cm ; Rate = 50cm/s

Data Collection:
- Piston Force (N)
- Piston Displacement (mm)
- Specimen Forces (N) and Moments (Nm)
- Specimen Acceleration (G’s)
- High-Speed Video

TASK 6 LOWER EXTREMITY STUDIES

Injury Review.

Field data analysis has been undertaken in collaboration with research personnel at the USAARL Injury Biomechanics Branch. The aggregation and synthesis of data has been an iterative process, as only military personnel have been provided with access to medical records contained within JTAPIC. Using an "underbody blast" exposure as an inclusion criterion, this dataset contains warfighter injury data from approximately 500 wounded-in-action (WIA) casualties and approximately 125 killed-in-action (KIA) casualties. Of these WIA warfighters, almost 200 sustained injuries to the foot/ankle. This region represents the most common injured region for WIA and a substantial problem for KIA as well. With regard to specific injuries, this data included at least 56 incidences of pilon fractures to the distal tibia, at least 57 incidences of talus fractures, and at least 100 calcaneus fractures. In addition, frequent notations of other distal tibia fractures, e.g., malleolar fractures, indicate that multiple foot/ankle prepositions may be represented within the dataset. Continued quantitative analysis will be pursued in close collaboration with USAARL Injury Biomechanics Branch personnel.

Non-destructive testing.

A pendulum experimental apparatus has been assembled to axial load lower leg specimens. This device consists of a 24 kg pendulum suspended from the ceiling and a freely moving mini-sled apparatus. The leg specimen is mounted to the sled system horizontally such that the incident pendulum face strikes the plantar surface of the foot following which the specimen travels down the sled rails. Load cells are mounted behind the pendulum face and at the specimen mounting location at the knee. The combined sled and specimen system was ballasted to 16 kg to maintain realistic inertial response. This device will be employed for low and medium velocity experiments. A pilot series of experiments was conducted using this device to ascertain the dependence of forces and moments at the knee to foot preposition at the ankle joint. These tests we conducted using the Hybrid 3 legform, which permits only flexion motions about the ankle. A rubber pad of 1.0 cm thickness was chosen to represent an arbitrary boot sole. Three positions were considered: neutral ankle, i.e., foot 90 degrees with respect to the tibia; 30 degrees plantar-flexed ankle, and 30 degrees dorsiflexed ankle. With each of these prepositions, the leg was axially loaded with the pendulum traveling at a velocity of 1.0 m/s, 2.0 m/s, or 3.0 m/s.

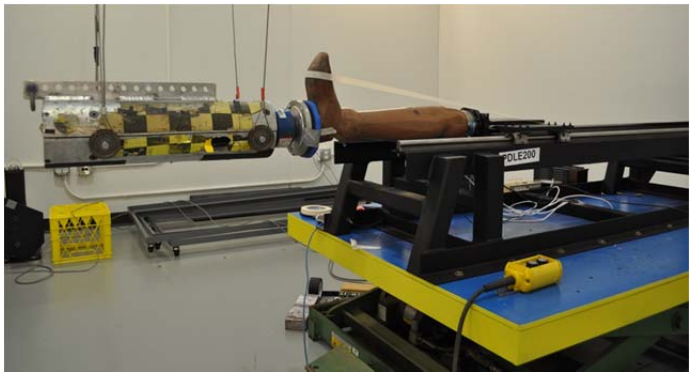

Experimental apparatus for axial lower limb loading; a Hybrid 3 legform is shown.

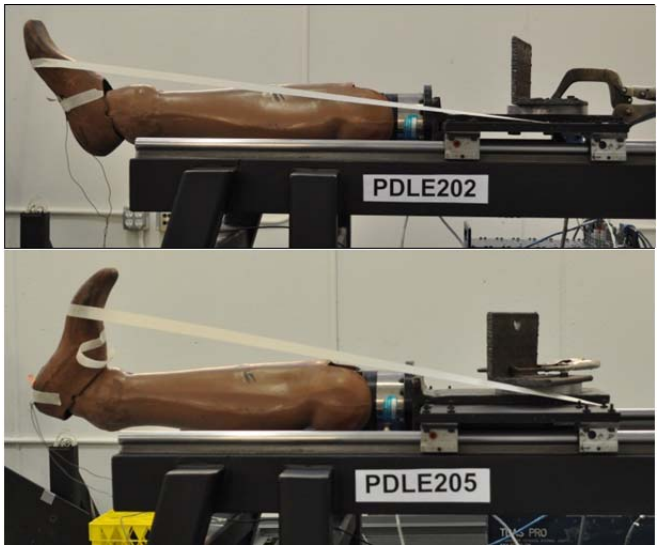

Ankle positioned in plantar-flexion (upper) and dorsiflexion (lower) for pilot axial loading tests.

Time traces from tests indicated that ankle prepositioning is an influential parameter in force and moment transmission to the upper tibia. When the foot was plantar-flexed, peak forces were reduced but duration of force application was extended. This did not necessarily suggest that this scenario was somehow protective. Rather, this was primarily due to the inertial response of the oblique plantar surface conforming to the vertical pendulum face. With regard to moment response, dorsiflexion reversed the direction of the upper tibia moment in the flexion/extension direction. Because of the asymmetrical cross section of the tibia, this reversed moment direction may translate to a reduced loading tolerance of the lower limb.

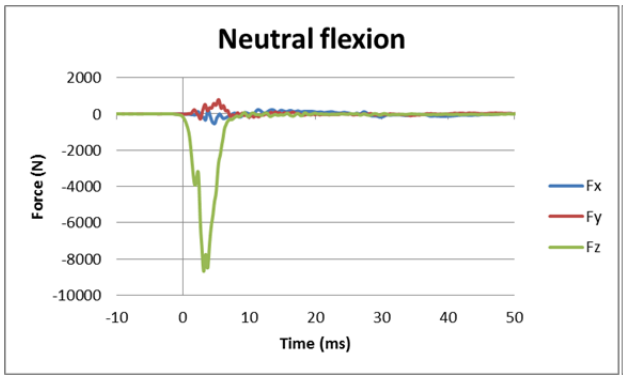

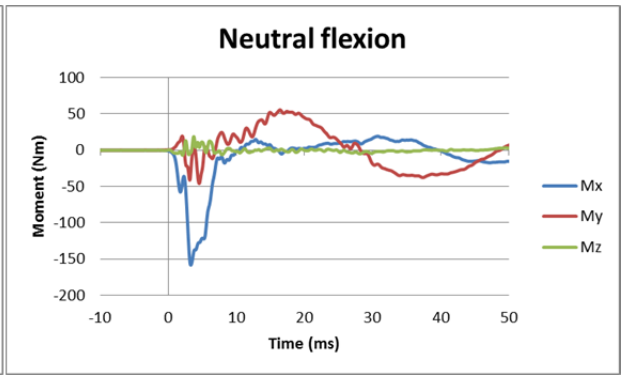

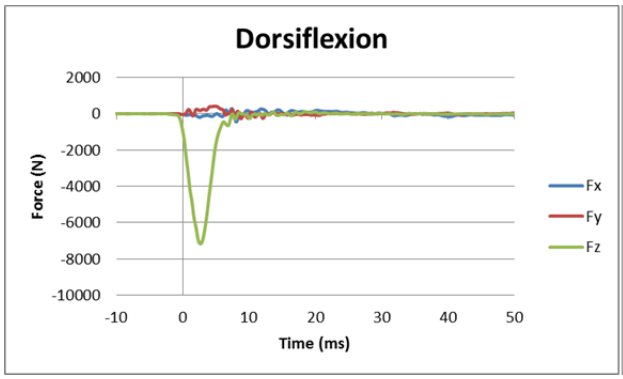

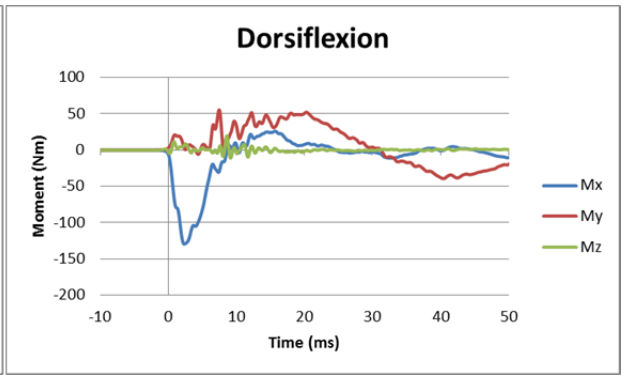

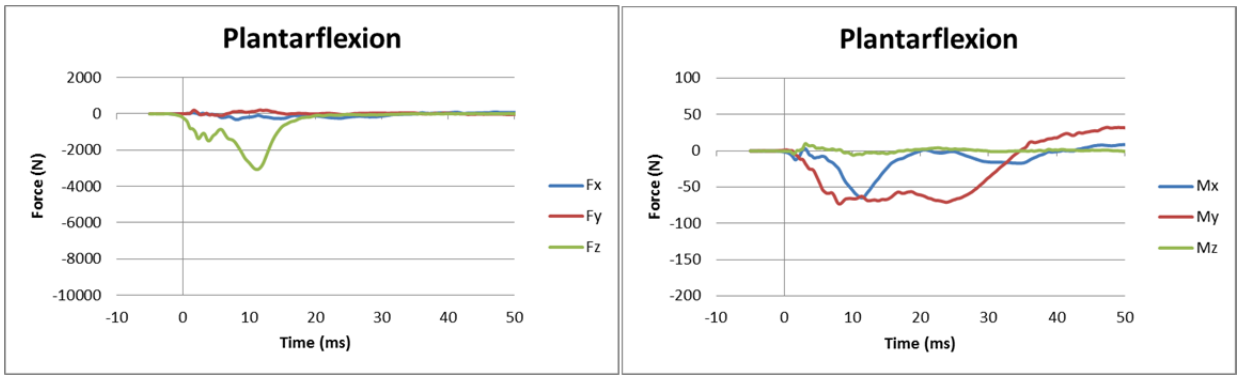

Time traces of forces (left) and moments (right) at the knee resulting from pendulum impact to the plantar surface of the foot at 3.0 m/s.

Two observations were made during this preliminary test series. First, that the vertical pendulum face may require some form of interface to ensure a force transmission to the leg which is more realistic compared to warfighter exposure in underbody blast. This interface will resemble a wedge to provide a vertical pendulum striking face and an angled foot contact face. Second, the sliding leg mount design requires further modification. Following contact with the low velocity (3.0 m/s) pendulum, the inertial run-out length is exhausted and the sliding mount contacts the track backstop. At velocities greater than those employed in this preliminary testing, the impact at the track backstop will increase in severity. The modified test apparatus includes frictional brushes along the length of the track run-out to dissipate energy and reduce the velocity of the slider prior to contacting the backstop.

Match-pair loading of MIL-LX

The approved budget for the Lower Extremity studies includes sufficient funding to purchase THOR-LX and MIL-LX devices. These items (two legs each) were ordered from Humanetics in October 2011. According to the manufacturer, these items have a delivery date nine months from order. We have recently received one pair of legs and await the second pair. Following the acquisition of these devices, matched pair testing will commence in identical testing fixtures employed for the PMHS experiments. We await Army approval of PMHS test protocol.

KEY RESEARCH ACCOMPLISHMENTS

- The scientific literature supports the notion that chronic exposure to the extreme environment of high performance aircraft flights appears to have a significant impact on the development of premature cervical spine degenerative changes. Several studies also confirmed the domination of age-related responses.
- A summary of in vitro biomechanical studies and computer modeling studies of cervical artificial discs revealed that an unconstrained device might relieve adjacent level stresses better than a constrained device, but more in depth analysis is needed.
- An in vivo animal study is underway that will compare two artificial disc models from two separate companies. The biomechanical aspect of the study will, for the first time in the literature, compare military-relevant loading between the two devices.
- A cervical spine computer finite element model was expanded in LS-DYNA software. Simulations were conducted and adjustments were made to the model so that it is currently validated against experimental data in flexion, extension, lateral bending and axial torsion.
- Current ATD designs of the lumbar spine have been mainly concerned with mimicking bending stiffness and not compressive stiffness of the human.
- The most widely used injury criteria for the lumbar spine used in the military is the Dynamic Response Index (DRI) that has several limitations including a limited validation set and untested assumptions about body position and external forces.
- A test buck for a programmable acceleration sled was designed and built to assess pelvic and lumbar spine dynamic compressive response in both ATD's and post mortem human subjects.
- Tests conducted on the Hybrid-III ATD with both curved and straightened lumbar spines demonstrated that forces further away from the source of impact were less sensitive to changes in impact pulse configuration.
- Hybrid-III ATD tensile loads measured in field blast tests are likely due to dummy design of the relatively stiff pelvis structures.
- PMHS (human cadaver) studies were done to assess lumbar spine fracture under vertical seat-pan loading. Studies indicated that acceleration pulse is a critical determinant of what body region fractures. Softer seats that generate a sigmoid pulse to the pelvis may protect the pelvis but contribute to lumbar spine fracture risk.
- Seat pan force magnitude may not be a good indicator of pelvis fracture.
- Current ATD lower limb designs have not been tuned to higher loading rates that accommodate both compression and a bending moment due to non-axial loading.

REPORTABLE OUTCOMES:

- Four quarterly reports of research progress submitted to COR
- Cochran J, Baisden JA, Yoganandan N, Pintar FA: Effects of Treatment for Cervical Disc Degenerative Disease in Military Populations. ASME IMECE conference paper 2011.
- Rangarajan N, Moore J, Gromowski P, Rinaldi J, Yoganandan N, Maiman DJ, Pintar FA, McEntire BJ: Response of dummies to high onset Gz loading on a sled. Accepted for poster presentation at Personal Armour Systems Symposium, PASS, conference. Nuremburg, Germany. September, 2012)
- A Post-doctoral fellow, Jason Hallman, was training under the direction of the PI and after one year of training, accepted a permanent position with Toyota at the technical research center in Michigan.

CONCLUSION

The research is still in progress. Literature reviews have provided specific directions for future experimental design. This information has been used to design an in vivo animal study to compare two different artificial disc surgical interventions against the current standard of care, bony fusion. The animal study protocols have been fully approved and are well under way.

Literature reviews have also provided direction on the lumbar spine studies and evaluation of current dummy designs is ongoing. The Army MIDAS dummy and the advanced THOR dummy have been recently included in the test matrix. Preliminary testing of five PMHS has described the nature and tradeoff between lumbar spine fractures and pelvic fractures. Dummy designs in general have spinal columns that are much less decoupled compared to PMHS.